**Lund University**

# *In Vitro* Studies on the Uptake of Ion-X-Gel Precursor and SPIO by Various Cell Types

Hampus Lundqvist

Master's degree in molecular biology, 45 credits
Spago Imaging AB and
Department of Biology, Lund University

# Table of Contents

# Abbreviations

**APTMS** - 3-Aminopropyl-Trimethoxysilane

**CT** - X-ray Computed Tomography

**DAB** - 3,3'-Diaminobenzidine

**DLS** - Dynamic Light Scattering

**DMEM** - Dulbecco's Modified Eagle Medium

**ELSD** - Evaporative Light Scattering Detector

**EPR** - Enhanced Permeability and Retention

**FBS** - Fetal Bovine Serum

**Fe** - iron

**HASMC** - Human Aortic Smooth Muscle Cells

**HeLa** - Human cervical cancer cell

**HepG2** - Human Hepatocellular carcinoma cell line

**HMEC** - Human Mammary Epithelial Cells

**HPLC** - High-Performance Liquid Chromatography

**HUVEC** - Human Umbilical Vein Endothelial Cell

**ICP-AES** - Inductively Coupled Plasma Atomic Emission Spectroscopy

**IgG** - Immunoglobulin G

**IXGp** - Ion-X-Gel precursor

**Jurkat** - Immortalized human T lymphocyte

**L929** - Immortalized mouse fibroblast

**MDA-MB-231** - Human breast carcinoma cells

**MRI** - Magnetic Resonance Imaging

**NMR** - Nuclear Magnetic Resonance

**NMV** - Net Magnetization Vector

**NSF** - Nephrogenic Systemic Fibrosis

**P** - phosphate

**PANC1** - Human Pancreatic Carcinoma cells

**PBS** - Phosphate Buffered Saline

**PEG** - Polyethylene Glycol

**PET** - Positron Emission Tomography

**RAW264.7** - Immortalized mouse macrophage

**RES** - Reticuloendothelial System

**RF** - Radio Frequency

**RPMI** - Roswell Park Memorial Institute medium

**Si** - silicon

**SPIO** - Super-Paramagnetic Iron Oxide

**$T_1$** - Time constant for recovery of NMV back to longitudinal plane

**$T_2$** - Time constant for NMV decay in the transverse plane

## Abstract

Contrast agents for MRI can greatly improve the contrast in the image, making it easier to pinpoint the position of, for example, inflamed tissues or tumors. There is a need for novel contrast agents with better spatial resolution, higher sensitivity, fewer false positives and lower toxicity. As for all pharmaceuticals, it is important to thoroughly test the compound prior to clinical applications.

The contrast agent IXG, currently under development by Spago Imaging AB, was analyzed *in vitro* for cellular uptake and toxicity. In order not to complicate future patents, a precursor was used. Viability analysis of HepG2, L929, RAW264.7 and Jurkat cells showed no apparent toxicity at concentrations above what is clinically relevant, while HUVEC cells were more affected. Cellular uptake was analyzed by ICP-AES and complemented with immunocytochemical staining.

An internalization of IXGp was seen in RAW264.7 cells and possibly, but not confirmed in Jurkat cells, but only when the cells were incubated with high concentrations. No uptake could be proven in HUVEC, HepG2 and L929 cells. The findings in this report can help in forming hypothesis on how IXG behaves in *in vivo* and may be useful for further developing the nanomaterial.


## Introduction

More than 10 million people around the globe were expected to be diagnosed with cancer in 2008[1]. Factors contributing the most to cancer are unhealthy food, smoking and infections. Other causes of cancer include radiation, stress, lack of physical activity, genetic heritage and pollutants[1]. It is estimated that in 2014 about 1.5 million people in USA will be diagnosed with cancer and about 600 000 will die within the year[2]. Breast cancer is the most common cancer form in American women and prostate cancer is the most common for men. Cancer in the lung and bronchus area is the second most common type, but it is the cancer form that claims most lives[2]. Reliable detection methods are important in order to be able to treat the disease in an early stage. Some methods for detection include CT, PET and MRI and methods for treatment are for example surgery, radiation- and chemotherapy[3]. Compared to two commonly used non-invasive imaging methods, CT and PET scans, radiation is not used in MRI and the spatial resolution of the image is still good[4].

## *Magnetic Resonance Imaging*

MRI is based on the quantum mechanical spin and positive charge of protons, which turn them into tiny magnets. If an external magnetic field, denoted $B_0$, is applied on a solution, a small excess of the proton spins will align with the $B_0$ field, forming the so called NMV. Individual spins will be turning around $B_0$ at a certain frequency ($\omega$). This frequency falls within the RF range and short, external RF pulses can force a small excess of the spins to change direction and start to turn around in the transverse plane instead, 90° to the $B_0$ field. The spins will start to relax and return to the longitudinal plane. The term used for the recovery process back to the longitudinal plane is called spin-lattice relaxation and the time constant for the process is denoted $T_1$. The process of decay in the transverse plane is called spin-spin relaxation and the time constant for this process is called $T_2$. In the $T_1$ recovery process energy is transferred from the nuclei to the environment, while in the $T_2$ decay process, energy is exchanged between nuclei. The NMV is detected with a receiver coil placed in the transverse plane, which registers the voltage that is created when the NMV in the transverse plane moves across the coil. It is possible to create contrast in images of the body because different tissues have different relaxation times and thus different signal intensities. For example, the molecular tumbling in water is much higher than in fat, and this makes the recovery of the NMV in water less efficient, resulting in a longer $T_1$.[4]

If this natural differences in contrast is not enough for a good image, one can use so called MRI contrast agents which can either increase or decrease the relaxation times, significantly improving the contrast in the images. To reduce the toxicity and tumbling rates $T_1$ enhancing agents can be bound to macromolecules or cheleated to organic ligands[5]. A water molecule that binds to the agent will tumble with it and be exposed to randomly oscillating magnetic fields. This stimulate to longitudinal relaxation and thereby shortens the $T_1$. Water molecules bind and dissociate with the contrast agent, allowing the effect to be spread out in the solution[5]. The local magnetic fields of $T_2$ enhancing agents affect the relaxation processes of the protons in water molecules nearby, resulting in shorter spin-spin relaxation time ($T_2$)[6]. Contrast agents are for example based on chelated gadolinium ($Gd^{3+}$), iron ($Fe^{3+}$), or manganese ($Mn^{2+}$)[4].

## *Contrast Agents*

Of all the MRI procedures done today, about 35 % include contrast agents[7]. There are two groups of contrast agents, the paramagnetic compounds that primarily reduce the $T_1$, giving a brighter image,

and the super-paramagnetic nanoparticles, which shorten $T_2$, resulting in a darker image. Gadolinium and manganese, belong to the first group while iron oxides fall into the second group. The main factors that determine how much a contrast agent can affect the relaxation rate are its size and chemical composition[8]. With its advantageous properties, the focus in this field has mainly been on gadolinium complexes. The metal displays high para-magnetism due to its seven unpaired electrons, has long electronic relaxation time and form very stable complexes with for example the ligand polyaminopolycarboxylate[7]. However, patients who are injected with gadolinium have a risk of developing NSF and nephrogenic fibrosing dermopathy, especially if they already have an impaired renal function[8]. Manganese is one of the first paramagnetic agents evaluated in hepatic and cardiac MRI, but the coordination number is 6, making it difficult to form very stable complexes with one or more water molecules[7].

By designing contrast agents in the nanorange size one can make use of the EPR effect to specifically target the agents to tumors. Nanoparticles used as contrast agents are often coated with different molecules to improve its functions and shield it from the immune system[9].

## *The Enhanced Permeability and Retention Effect*

Pharmacological molecules can be targeted to to tumors by the EPR effect. This effect happens because tumors that reaches sizes of 150-200 µm begin to stimulate the formation of new blood vessels to support their increasing demand of oxygen and nutrition[10]. The structure of these tumor blood vessels is rarely very good since they often lack a smooth muscle layer and consist of badly aligned and defective endothelial cells, resulting in unusual wide fenestrations[10]. The lymphatic drainage is ineffective in tumors, a factor that allows the particles to remain in the tumor for a longer time[10]. Therefore, the molecular- and fluid transportation will be abnormal within the tumor. Thus, by creating a nanomaterial of just the right size, it will have the potential to circulate in the blood until it reaches the tumor where it can exit the blood stream via the abnormal blood vessels and then remain in the tumor for a longer time.

## *Ion-X-Gel*

Since many of the commonly used contrast agents today may cause NSF and are prone to generate, there is a need for new types of contrast agents. Spago Imaging AB is currently developing a novel

nanosized contrast agent with potential for greater spatial resolution and fewer false positives and side effects. Their goal is to produce a cost effective product that makes it possible to locate soft tissue cancers at an earlier stage than currently possible, thereby lowering the suffering and treatment time for patients. One of the particle's advantages is that it can easily be customized. The surface can for example be treated in different ways and the size can be modified, allowing the particle to be directed at specific target tissues and having the desired cellular interaction. The core particle is a biocompatible nanomaterial called Ion-X-Gel, consisting of cross-linked, silicon based polymers with a PEGylated surface. By embedding paramagnetic manganese into the polymer framework the resulting relaxivity is six times better than the currently available gadolinium-based contrast agents[11]. The nanomaterial will be injected into the blood stream where it will circulate until it reaches the leaky blood vessels of the tumor tissue where it will enter the tumor and accumulate via the EPR effect. To be able to publish this work without ruin future patents, experiments were done using a precursor of IXG, without manganese.

## *Nanoparticle Coating*

Nanoparticles can be coated with repeats of ethylene ether to make them less prone to interact with surrounding molecules and cells. The PEG units form a passive surface on the particles and reduce the risk of aggregation, which otherwise could lead to capillary occlusion and trapping the particles in for example the lungs and liver[9]. PEGylated nanoparticles are also better shielded from uptake via the RES system, allowing them to remain in the circulation for a longer period, rather than being transported to the spleen and liver[9]. Charge interactions with proteins and small molecules are also reduced, while the solubility in buffer and serum is increased because of the hydrophilic properties of the PEG[9]. PEGylation is FDA approved for a large range of applications and often cheap[9].

## *Nanoparticle Size and Structure Influence Uptake*

The size and surface functionalization of nanoparticles affect their rate of internalization in cells. Increasing size has been reported to both increase and decrease uptake. Doiron *et al.* (2011) showed that, in HUVEC cells, 20 nm polystyrene spheres were adhered and internalized 300 times more effective than 100 nm particles[12]. On the other hand, when the cells were grown in a 3D collagen hydrogel, larger particles up to 500 nm were internalized faster[12]. Another study on Jurkat and PANC1 cells using 10 – 100 nm gold particles revealed a higher cellular uptake with increasing

particle size[13]. The PANC1 cells were reported to internalize the particles more effective than Jurkat[13]. SPIO particles of 20 – 150 nm has been seen to be taken up more effectively by human monocytes if the particles are larger and if functionalized with ionic carboxy groups, they were also taken up better than non-ionic particles[14]. Saito *et al.* (2012) reported that mouse macrophages (RAW264) cells internalized alkali-treated dextran magnetite more effectively than dextran magnetite coated with carboxymethyl[15]. A study showed that non-functionalized polyisoprene nanoparticles were taken up by Jurkat and HeLa cells more effectively compared to other polymeric particles[16].

## *The Current Study*

It is important to evaluate and learn how medicals behave in a living organism. Any newly developed molecule or particle that is to be in contact with the human body must be thoroughly tested prior to clinical applications. In this project the interaction of IXGp with different cells has been studied with focus on internalization of the nanoparticles and their toxicity. The experiments were carried out *in vitro* as one of the first steps to forming hypothesis about how the particles might behave in *in vivo* systems. The ideal IXG nanomaterial would have a very limited toxicity and would only be taken up by cells to a low degree, allowing it to stay in the blood stream for a longer time. Four immortalized cell lines, HepG2, Jurkat, L929 and RAW264.7, as well as the non-immortalized HUVEC cell line were exposed to various concentrations of IXGp for 24 hours. CellTiter Blue fluorescence was used to determine the metabolic activity of the cells, as a measurement of viability. The amount IXGp taken up in the cells was determined by measuring the silicon content using ICP-AES and the experiments were complemented with immunocytochemical staining. SPIO particle were used as a positive control for nanoparticle uptake, as many cell types are known to internalize the particles[14]. Uptake of SPIO was analyzed with a NMR 60 μMz relaxometer and confirmed with Prussian Blue staining.

# Materials and Methods

## *Preparation of IXGp*

PEGylated IXGp was isolated from a crude production batch made by Spago Imaging AB. The correct particle size was isolated by filtration as follows. The particles were first prefiltered through a 0.45 μm Rapid-Flow filter (Nalgene) and then through a 300 kDa laminar flow filter (Pall) together with a double volume of 150 mM NaCl. The permeate was again diluted with a double volume of 150 mM NaCl and was then filtered on a 10 kDa laminar flow filter (Pall). The retentate was collected and filtered through a sterile 0.2 μm Supor membrane (Pall) to remove dust particles. The particles were electrolyte balanced using a confidential method. The pH was adjusted to 7.4 with 1 M NaOH and the osmolality was determined using a Vapor Pressure Osmometer (Wescor). The sizes of the crude and filtered particles were determined using HPLC (Chromtech) with a gel filtration column (Pharmacia) and an ELSD 2000 (Alltech). The IXGp concentrations was determined by measure the silicon content using ICP-AES. A chromogenic Limulus Amebocyte Lysate test (Lonza) was used by Spago Imaging AB to verify that endotoxins were not present. Unless otherwise stated, all IXGp particles used were electrolyte balanced.

## *Preparation of SPIO Particles*

### PEGylation of SPIO

Pure super-paramagnetic iron (II, III) oxide nanoparticles in aqueous solution with a size of 10-12 nm (ABCR, Germany), in six different concentrations (0.9 - 2149 mM Fe) were incubated for 1-2 days with 0.35 or 2.4 M PEG 1000 (Fluka, Germany) and were then diluted to a series of different concentrations (0.9-358 mM Fe) in distilled water. Non-PEGylated SPIO (naked SPIO) was used as controls. The solutions were sonicated for 20 min at 37 °C using a Ultrasonic Cleaning Bath (Branson) and were then filtered through a 0.2 μm Supor syringe filter (Pall).

PEGylation was also done on 4.8 nm SPIO nanoparticles stored in toluene (Sigma-Aldrich) following the methods used by Ma *et al*[17]. SPIO and PEG 1000 were mixed together in dichloromethane, giving final concentrations of 8 mM Fe and 0.45 mM PEG 1000. The SPIO was

slowly diluted to 2 mM Fe in DMSO. Attempts to concentrate the particles were first done by centrifugation at 1610 x g for 2 minutes and then by washing with milli-Q water 8 times while placed on a strong magnet.

Prior to DLS analysis (see section Stability of Nanoparticles), unattached PEG molecules were removed from the SPIO particles by spin filtration at 10 kDa (Amicon Ultra, Míllipore). The solutions were filtered 4 times at 12 000 x g for 10 min, discarding flow through. For SPIO PEGylated at 2.4 M PEG, surplus PEG was more difficult to remove since the solution was too viscous for filtration with a spin filter. Thus, the samples were diluted in water and centrifuged at 920x g for 5 min to spin down the heavier particles, separating them from the lighter PEG units. The particles were then filtered with a centrifugal filter of 10 kDa (Amicon Ultra) at 5525 x g for 20 min. The retentate was washed 8 times with 4 ml water by centrifugation as above. Naked SPIO were filtered through a 0.2 µm Supor syringe filter (Pall).

## Coating of SPIO with APTMS

SPIO in aqueous solution was diluted to 215 mM Fe in 70% EtOH or MetOH and was sonicated in water bath for 1 hour at roughly 37 °C. APTMS (Aldrich) was added to a final concentration of 0.2 or 0.4 %. The samples were sonicated for 2 hours and nitrogen gas was blown on the solutions for 10 min to remove the alcohol. The particles were dried either overnight at 50 °C or for 2 hours at 50 °C and then at room temperature for three days. The particles were resuspended in distilled water to three different concentrations of Fe (54 - 430 mM), sonicated for 2 hours and filtered through a 0.2 µm Supor syringe filter (Pall). The presence of APTMS on the SPIO particles was verified with ninhydrin staining (Sigma-Aldrich); using glass capillaries, APTMS coated SPIO was spotted on a filter paper and a ninhydrin solution of 1.4 M in 99.5 % EtOH was placed on top. Naked SPIO of 197 mM Fe in 70% EtOH and 0.4% APTMS in 70% EtOH were used as controls. A purple color signifies the presence of APTMS as ninhydrin reacts with amines and forms a colored product.

## *Stability of Nanoparticles*

PEGylated, APTMS coated and naked SPIO were diluted to 0.22-90, 0.25–72 and 0.2 - 120 mM Fe, respectively in distilled water, 0.9% NaCl, RPMI- and DMEM cell culture medium, all four solutions with and without 10% FBS supplementation. After incubation for two hours at room

temperature, the solutions were visually examined for any signs of aggregation or changes in color. IXGp could not be tested in this way due to a similar diffraction index as water.

DLS analysis was done to see how the IXGp and SPIO particles behave in different solutions regarding size and particle aggregation. PEGylated and naked SPIO particles were diluted to 1 - 36 and 1 - 7 mM Fe, respectively, in DMEM cell culture medium with 10% FBS, distilled water and PBS. IXGp solutions of 21 - 107 mM Si were filtered at 0.2 µm and measured in DMEM- and RPMI cell culture medium with 10% FBS, and in milli-Q water, 150 mM NaCl, and PBS. DMEM and RPMI with and without 10% FBS, and distilled water were used as blanks. Non-electrolyte balanced IXGp were tested using the same parameters.

## *ICP Analysis*

The concentrations of Fe in PEGylated and naked SPIO, of Si and P in IXGp stock solutions, and of Fe and Si in cells treated with SPIO and IXGp, respectively, were determined by ICP-AES at the Plant Ecology laboratory, Lund University. Prior to analysis, SPIO solutions and cells exposed to SPIO were diluted in 6 M HCl, while cells incubated with IXGp were first diluted in 4 M KOH where after the pH was adjusted to roughly 12 using 6 M $HNO_3$. The personnel at the ICP facility used 0.02 M $HNO_3$ or 12 M HCl to further dilute the samples to appropriate concentrations.

## *Cell Cultures*

Cell cultures were maintained in 75 $cm^2$ flasks at 37 °C, 5% $CO_2$, 95% humidity, and were subcultured about 2 times a week when reaching 80% confluency. HepG2 and L929 cell lines were grown in DMEM (HyClone) medium and Jurkat and RAW264.7 in RPMI 1640 (HyClone) medium. Both media where supplemented with 10% FBS (HyClone) and penicillin-streptomycin solution (10 000 U penicillin/ml, 10 000 ug streptomycin/ml, HyClone). HUVEC cells were grown in Medium 200 with Low Serum Growth Supplement (Life Technologies), 5 mg gentamicin/ml and 125 µg amphotericine B/ml (Life Technologies). Bürker cell counter were used to determine cell number.

Growth curves and toxicity tests were carried out in 96 well-plates with black or clear walls, by seeding 2000-10 000 cells in 90 µl/well. Nanoparticle uptake and staining tests were performed in 6 well-plates by seeding $5x10^5$ cells in 3.6 ml/well. After being seeded, the cells were allowed to settle

for one day and were then treated with nanoparticles for 16-24 hours before being further analyzed.

## *Cellular Growth Curves*

Growth curves were established by seeding 2000 - 10 000 HepG2 and Jurkat cells in 90 µl/well in 96 well plates. At 0, 20, 44, 68 and 92 hours after seeding, 10 µl CellTiter Blue (Promega) was added to 6 wells for each cell type and to 1 well with medium (blank). The fluorescence was measured 4 hours after addition of CellTiter Blue at Ex560 nm and Em590 nm using a fluorescence plate reader, FLUOstar Galaxy (BMG Labtechnologies).

Total fluorescence as a function of cell density was determined by making dilutions series and seeding 781 - $10^5$ Jurkat cells in 8 different concentrations in 90 µl/well to 6 wells/concentration and measuring fluorescence 4 hours after the addition of CellTiter Blue.

## *Toxicity of SPIO and IXGp*

HepG2, Jurkat, RAW264.7, L929 and HUVEC cells were seeded at 5 000 or 10 000 cells in 90 µl/well in 96 well plates with black or clear walls, incubated overnight and were then treated with 4 - 7 different concentrations of naked SPIO (0.05-1.8 mM Fe) or 5 different concentrations of IXGp (0.5- 21 mM Si). Cells were also incubated with 5 mM Si (IXGp) that had not been electrolyte balanced. After 24 hours incubation with particles 10 µl CellTiter Blue (Promega) was added to the cells, and after another 4 hours the CellTiter Blue fluorescence was measured at Ex560 nm and Em590 nm using a FLUOstar Galaxy (BMG Labtechnologies).

To see if potential toxicity was time dependent 1.8 mM Fe (naked SPIO) or 21 mM Si (IXGp) was added to cells 4 hours before measurement and compared to 24 hours incubation. Particles added 5 minutes prior to measurement was used as a control to rule out any particle interference on already formed fluorescent product. Cell culture medium with particles, but without cells was used as a control and cells treated with only milli-Q water was used as another negative control.

## *Uptake of SPIO and IXGp*

HepG2, Jurkat, RAW264.7, L929 and HUVEC were seeded at $5x10^5$ cells in 3.6 ml/well in 6-well plates and incubated overnight. They were then treated with 0.036, 0.358 and 0.895 mM Fe (naked

SPIO) or 0.5, 2 and 21 mM Si (IXGp), in triplicate wells. Medium with particles but without cells was used as one type of negative control and cells treated with milli-Q water as another. Naked SPIO of 0.895 mM Fe was used as positive reference controls in IXGp uptake tests. After 24 hours incubation, the cells were washed 3 times with 4 ml medium or PBS. The cells were trypsinized with 400 µl trypsin. For HUVEC cells, 0.5-1 ml trypsin/EDTA (Gibco) was added for 1 min at room temperature and 2 ml trypsin neutralizer (Gibco) was used to stop the trypsinization. All cells, except Jurkat, were resuspended in 4-6 ml medium and were transferred to test tubes. The non-adherent Jurkat cells were instead pooled into tubes without trypsinization. The cells were centrifuged at 300 x g for 5 min and the pellets were washed 3 times with 5 ml PBS by vortexing briefly and centrifuging as above.

One SPIO uptake trial on HepG2 cells were done by seeding $5x10^5$ cells in 0.9 ml/well in 24-well plates. The final volume after addition of SPIO or $H_2O$ was 1 ml. Each well was washed 3 times with 200 µl PBS by pipetting and the cells were trypsinized with 200 µl trypsin. Medium of 0.5 ml was added to each well and 5 wells/concentration were pooled, giving triplicates of each concentration. The cells were centrifuged and washed as above, but using 3 ml PBS.

In all uptake tests, nanoparticle adsorption controls were set up where the highest concentrations of SPIO or IXGp were added to the cells 10 minutes before the washing steps. The cell density in each triplicate sample was determined using a Bürker counting chamber. Cells treated with IXGp were pooled into 1 tube per concentration and frozen until ICP-AES analysis.

## *Nuclear Magnetic Resonance Measurements*

The $T_2$ of cells treated with SPIO was measured the same day or a few days after the uptake tests, using a Minispec mq60 NMR broadband spectrometer (60 MHz, Bruker corporation) at 37 °C. The machine was set to measure 4 scans, sampling 200 data points, having a 20 sec recycle delay and a first pulse separator of 1 ms. A standard curve of $T_2$ versus SPIO concentrations between 3.5 - 895 µM Fe was measured in order to correlate NMR signal from cells incubated with SPIO to iron concentration.

## *Statistics*

Mean values from collected data, where possible, were calculated and presented with standard

deviations in graphs. Welch two sample t-test were used to test if data were significantly different. A value below 0.05 were viewed as significant.

### *Prussian Blue Staining*

HepG2 and RAW264.7 cells were seeded at $5x10^5$ cells in 3.6 ml/well in 6-well plates, incubated overnight and then treated with 0.9 mM Fe (naked SPIO) in triplicate wells. Medium with particles but without cells was used as one type of negative control and cells treated with milli-Q water as another. After 24 hours, the cells were incubated with 0.5 ml 4% formaldehyde for 40 minutes at room temperature, air dried for 20-35 minutes and incubated with 0.5 ml working iron stain solution (Accustain, Sigma-Aldrich) for 10 min at room temperature. Nanoparticle adsorption controls were set up where cells were treated with 0.9 mM Fe (naked SPIO) for 10 minutes before the washing and staining steps. The staining was done both with and without 0.5 ml Neutral Red counter staining for 1 min at room temperature. The cells were washed 3 times with 2 ml PBS before and in-between addition of each reagent, and once after Neutral Red counter staining. The stained cells were viewed with a microscope.

### *Immunocytochemical Staining*

HUVEC, RAW264.7, L929 and HepG2 cells were seeded at $5x10^5$ cells in 3.6 ml/well in 6-well plates, incubated overnight and then treated with 0.5, 2 and 21 mM Si (IXGp). Medium with particles but without cells was used as one type of negative control and cells treated with milli-Q water as another. Before and in-between addition of the following solutions, the cells were washed 2 times with PBS for 3 minutes by shaking at 200 rpm. The HUVEC cells were never exposed to shaking as they easily detached. The cells were fixated with 1 ml 4% formaldehyde for 20 minutes or with 0.5-1 ml 5% glacial acetic acid in 95% EtOH for 3-7 min and then treated with 0.5-1 ml 3% Tween 20 (Sigma-aldrich) for 10 min. Cells incubated with 21 mM Si (IXGp) but not permeabilized with Tween 20 were used as adherence controls. The cells were incubated with 0.5-1 ml 3% $H_2O_2$ in PBS for 10-15 min and then with 1-1.5 ml 1-5% FBS in PBS for 1-1.5 hours. The cells were then incubated with 0.5-1 ml 1 μg/ml rabbit-anti PEG-B-47 (Abcam) for 2 hours and were then washed with 4 ml 1% FBS in PBS for 3 min. Cells incubated with 21 mM Si (IXGp) but not exposed to anti-PEG were used as negative controls. The cells were incubated with 1 ml 0.4 μg/ml goat anti-rabbit IgG (H+L), conjugated with horseradish peroxidase (Pierce, Thermo Scientific) for 2 hours. The cells were washed with 1% FBS for 10 min and were then treated for 5-7 min with 1 ml DAB

substrate (Thermo Scientific) prepared according to manufacturer's instructions. The cells were washed 2 times with 4 ml PBS and were then viewed with a microscope. Nanoparticle adsorption controls were set up where cells were treated with 21 mM Si (IXGp) for 10 minutes before the washing and staining steps.

# Results and Discussion

## *Stability of SPIO*

Five different concentrations of naked SPIO were incubated for 2 hours in different solutions and visually examined for aggregates and color changes. No signs of aggregation was seen when diluting naked SPIO to 0.2 – 14 mM Fe in DMEM- and RPMI cell culture medium supplemented with 10% FBS. This gave a first indication that naked SPIO was stable enough in the cell culture medium, even at an iron concentration 16 times higher than used in the uptake tests. In DMEM without FBS, a lot of SPIO aggregation was observed at 5.6 mM Fe. Naked SPIO at 120 mM Fe formed aggregates in all solutions, except water, with the most aggregation in DMEM. A high degree of aggregation was seen when PEGylated SPIO were diluted in DMEM without FBS to 0.7 mM Fe, but very little aggregation was observed in DMEM supplemented with 10% FBS. No aggregates were seen in RPMI with or without FBS up to 9 mM Fe. PEGylation of SPIO in toluene did not work as the particles got stuck on the pipette.

SPIO treated with APTMS was rendered much more prone to aggregate compared to naked SPIO particles. In some cases aggregates were formed during the coating procedure and much of the iron was lost during filtration. Thus, even though the tests for the presence of APTMS using ninhydrin turned up positive, the method used for coating with APTMS did not work.

The notion that the PEGylation of SPIO did not work was confirmed with DLS. According to the manufacturer the SPIO particles should have a size of 10 - 12 nm, but as seen in figure 1, PEGtreated SPIO particles had a mean size of about 40 - 70 nm when diluted in water, 70 and 260 nm in PBS and 72 and 78 nm in DMEM (10% FBS). The two highest concentrations of SPIO, 10 and 40 mM Fe are estimates because the exact concentrations is not known since those solutions come from two different SPIO sediments of the same solution. It is unexpected that the lowest concentration of the two SPIO solutions in PBS have a much higher mean value, but seeing as the standard deviations is larger than the actual mean value it means that there are a large range of different sizes detected by the DLS apparatus which could mean that for example dust particles have entered the solution.

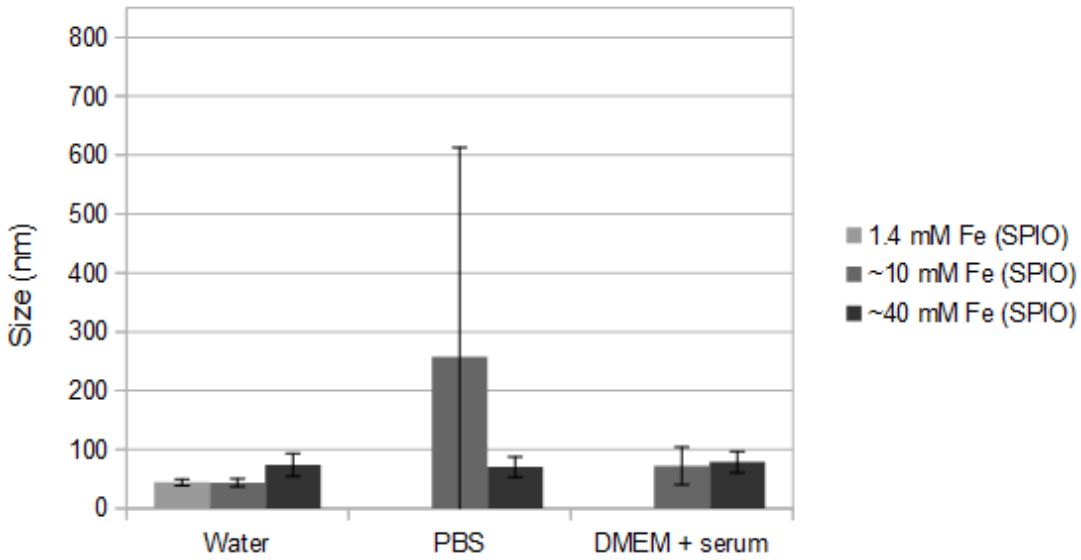


*Figure 1: DLS measurement of PEGtreated SPIO particles in water, PBS and DMEM (10% serum). Data is presented as mean values with standard deviations. The two highest concentrations here are estimates since those solutions come from two different SPIO sediments of the same solution.*

Figure 2 show DLS analysis of 1.9 and 9.6 mM Fe (naked SPIO) in water and 9.6 mM Fe (naked SPIO) in PBS and DMEM (10% FBS). In water the sizes are about 40 and 380 nm, and in PBS and DMEM (10% FBS) around 170 and 230 nm, respectively. The mean sizes of naked SPIO particles are generally higher compared to PEGtreated SPIO particles, but the aggregation is till high in PEGtreated particles as well. Since the coating of the SPIO particles did not work and since it was not the main goal in this project and time was limited naked SPIO particles were instead used in the uptake tests as no aggregates were seen during visually examinations of SPIO in cell culture medium supplemented with 10% FBS.

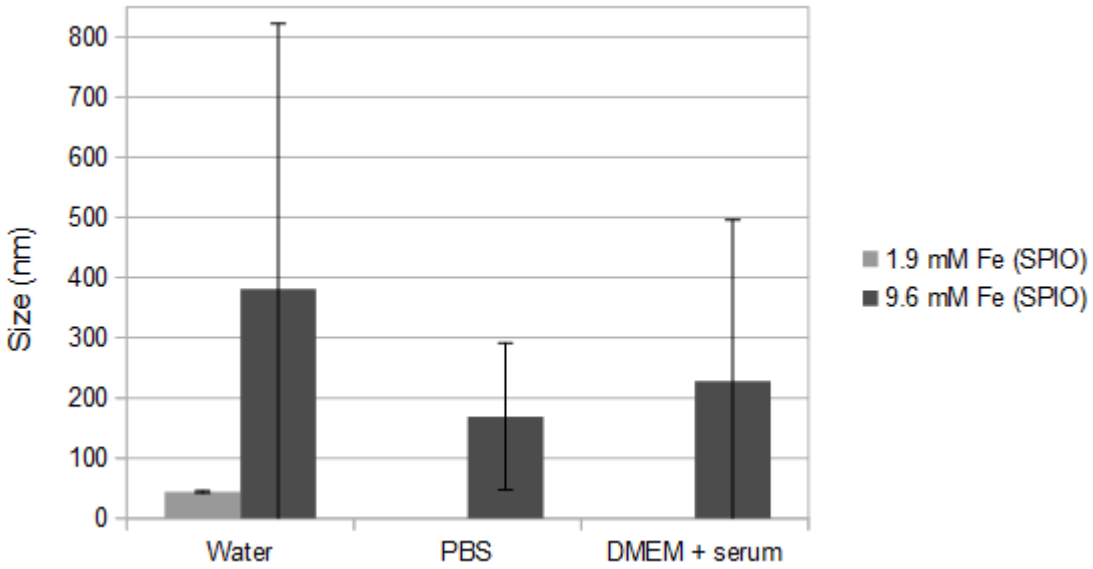


*Figure 2: DLS measurement of naked SPIO particles in water, PBS and DMEM (10% serum). Data is presented as mean values with standard deviations.*

The methods for PEGylation and APTMS coating were based on a previous project work at Spago Imaging AB, where magnetic iron (II, III) oxide (ABCR, Germany) in aqueous solution was successfully APTMS coated and PEGylated with PEG1000[18]. In the present project, the same type of SPIO particle was used, but for some reason the coating did not work.

## *Stability of IXGp*

Using HPLC (Chromtech) with a gel filtration column and an ELSD 2000 (Alltech) the size of the crude and electrolyte balanced IXGp particles was roughly determined to be between 4 and 6.5 nm (the sizes of the control proteins myoglobin and albumin) in an ammonium carbonate buffer of pH 7.4. There was no detectable difference in size if the particles were electrolyte balanced or not.

DLS measurements on non-electrolyte balanced IXGp diluted to 21 - 107 mM Si in water and NaCl and undiluted particles, 215 mM Si, can be seen in figure 3. The undiluted IXGp particles showed a size of 2.8 nm which decreased to roughly 2.3 nm in water, a phenomenon that has been seen before at Spago Imaging AB and is believed to be a combination of the particles being relative small and having a refractive index similar to $H_2O$, which make them difficult to detect when diluted. The particle sizes instead increased to 4.0 - 4.9 nm when diluted in NaCl which has also been seen before in reports from Spago Imaging AB. The larger size seen with the HPLC compared to the DLS on undiluted and water diluted particles could be explained by the ammonium carbonate buffer

containing ions, as ions could bind in the structure and cause an increase in size, similar to the increase in size of the particles diluted in PBS and NaCl solutions.

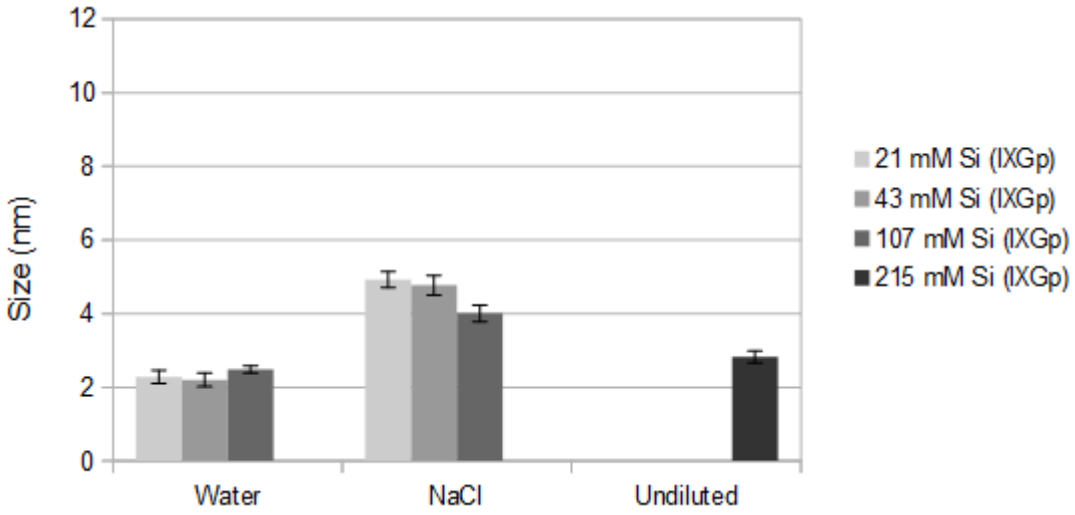


*Figure 3: DLS measurement on various concentrations of non-electrolyte balanced IXGp particles in water and NaCl. Data is presented as mean values with standard deviations.*

In figure 4 DLS measurements on electrolyte balanced IXGp particles, adjusted to pH 7.4 can be seen. The electrolyte balanced particle are in general larger, 7.1 nm as undiluted and decrease down to 4.9 nm when diluted in water. The size is marginally lowered to 6.9 in PBS while in RPMI (10% FBS) and DMEM (10% FBS) the sizes are larger, 7.8 and 10 nm, respectively. The larger size of the electrolyte balanced and pH adjusted particle could again be due to exposure to ions, for example during the pH adjustment. Exposure to more ions in the PBS solutions would not increase the size further if the particles were already saturated with ions. Seeing as RPMI (10% FBS) and DMEM (10% FBS) alone show sizes of 8.3 and 7.8, the apparent increase in size of IXGp when diluted in cell culture medium supplemented with serum could be an artifact caused by detection of the serum proteins. Over all, these results strongly suggests that the IXGp particles are stable in water, NaCl and cell culture medium.

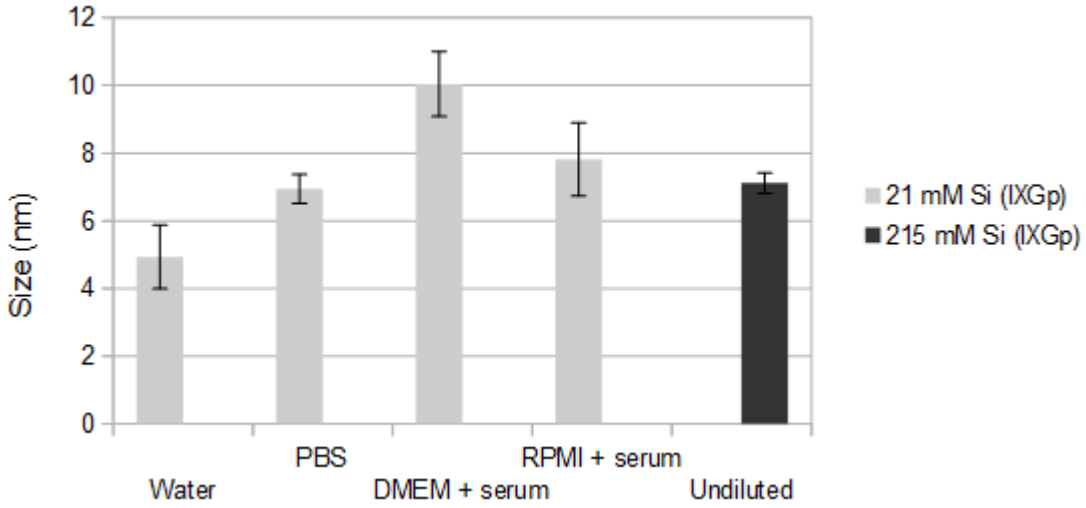


*Figure 4: DLS measurement on various concentrations of electrolyte balanced IXGp particles adjusted to pH 7.4. The particles were measured in water, PBS, DMEM (10% FBS) and RPMI (10% FBS). Data is presented as mean values with standard deviations.*

The osmolality of the IXGp particles were determined to 820 mosmol/kg $H_2O$ which is higher than the physiological value of about 290 mosmol/kg $H_2O$[19], but osmolality of up to 800 mosmol/kg $H_2O$ is tolerated for intravenous injections of smaller volumes[19]. To the author's knowledge, there is no easy way of lowering the osmolality and therefore it was decided to continue using these particles.

## *HepG2 and Jurkat Cellular Growth Curves*

The fluorescence seen when cells are treated with CellTiter Blue comes from the compound resorufin. Actively metabolizing cells convert the molecule resazurin, in the CellTiter Blue substrate, into resorufin. The total metabolic capacity determines the amount resorufin formed and thus, the fluorescent signal. In the cellular growth curves the increased signal over time has been interpreted as an increase in cell number, with the assumption that the cells had similar metabolic activity during the time interval. Figure 5 shows relative fluorescence of cells 4 to 96 hours after seeding 2000 Jurkat cells and 5 000 or 10 000 HepG2 cells. It appears that HepG2 cells immediately fall into a steady doubling time (assuming constant metabolic activity for each cell) which start to decrease a little after 24 hours if 10 000 cells were seeded. When seeding 2000 Jurkat cells, the doubling time is markedly slower, probably due to low cell concentrations which would lead to low contact based cell signaling, slowing down growth. The differences between the two HepG2 curves are significant for all time points except after 72 hours. Oddly, when seeding 5000 HepG2 cells, a plateau phase is reached after 72 hours, while the cells continue to grow if 10 000 cells were seeded

initially. On the other hand, the fact that the two growth curves with HepG2 cells appear to reach similar cell densities after 72 hours suggests that the initial higher cell number of 10 000 cells begins to hinder the growth as cells likely are reaching a high confluency.

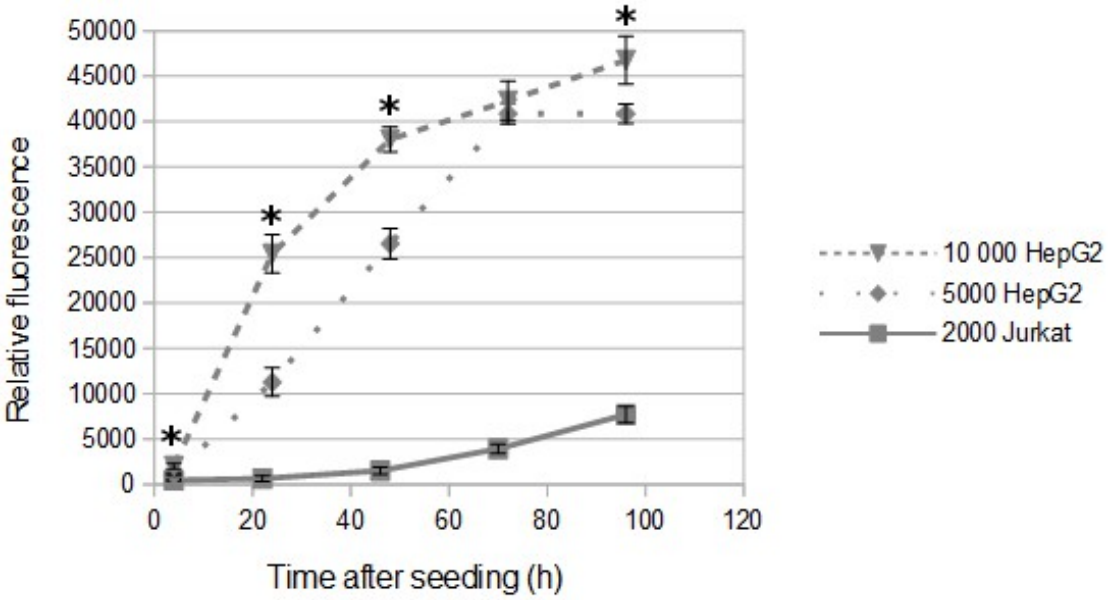


*Figure 5: Growth curves of Jurkat and HepG2 cells presented as mean relative fluorescence per hour +/- standard deviation. The initial cell number can be seen in the legend. Cells were cultured in 90 µl/well in 96-well plates, 6 replicates. The starts indicate a significant ($p<0.05$) difference between the three graphs at respectively time interval.*

During viability measurements on cells treated with SPIO or IXGp, 5000 or 10 000 cells were seeded in 96-well plates. Thus, these results suggests that HepG2 and presumably the other cell lines as well, were in growth phase during the viability tests (24-48 hours after initial seeding), since 5000 or 10 000 cells were seeded in 96-well plates for the viability tests. On the other hand, this data is more difficult to apply to the uptake tests because the cells were seeded in 6-well plates since only 96-well plates could be analyzed in the available fluorescence plate reader. The cells in the uptake tests were seeded at a concentration 6.25 times higher than the Jurkat cells in the growth curve and it looked like the cells had grown well when observed in a microscope. Since the growth curves were only a reference to verify at what growth phases the cells were in during the uptake test, growth curves were only created for two of the five cell types.

To determine how well the number of cells correlate with relative fluorescence, dilution series of Jurkat were done (figure 1, appendix 1). The number of Jurkat cells versus fluorescence gives a linear relationship up to 1800 relative fluorescence.

## *Toxicity of SPIO*

The metabolic activity of cells treated with naked SPIO is presented in figure 6 as percent fluorescence compared to control cells not treated with SPIO. Up to 1.8 mM Fe (naked SPIO) appear to have no negative effect on L929 and HepG2 cells, but instead increase the metabolic activity almost up to 120% of control. Jurkat cells instead show a slight, but significant decrease in fluorescence after 0.9 mM Fe, which then increased again at 1.8 mM Fe. The RAW264.7 cells show a drastic increased in florescence signal up to 160% of control at 0.9 mM Fe (naked SPIO) and then decrease slightly at 1.8 mM, but there is no significant difference between the two data points. The HUVEC cells here are very sensitive to the SPIO particles with a dramatic decrease in fluorescence signal.

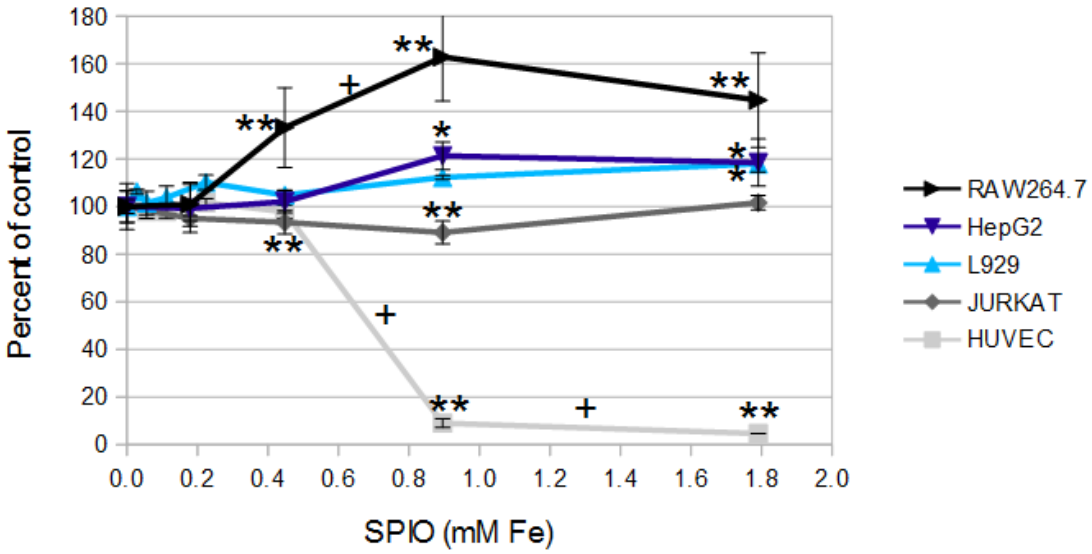


*Figure 6: Viability of cells incubated with various concentrations of SPIO over 24 hours, presented as mean percent of control +/- standard deviation. Control cells for each cell line were cells treated with only $H_20$. Cells were seeded in 90 µl//well in 96-well plates, 3 replicates. CellTiter Blue was added 4 hours before measurements. The stars show a significant difference (*: p<0.05, **: p<0.01) compared to control. A plus sign indicates a significant (+: p<0.05, ++:p<0.01) difference between two data points.*

Figure 7 shows metabolic activity in percent of control for cells treated with 1.8 mM Fe (naked SPIO) for 5 minutes, 4 hours and 24 hours. The fluorescence signals are significantly increased for RAW264.7 and L929 cells compared to control, at all data points. It should be noted that only 1-2 replicates were made for Jurkat and HepG2 cells incubated for 5 minutes and 4 hours and thus neither standard deviation nor a significant value can be calculated, however these two cells types show a fluorescent signal closer to the control value than the other cell lines, thus appear to be less

affected by SPIO. The HUVEC cells here are very sensitive to the SPIO particles already after 5 minutes.

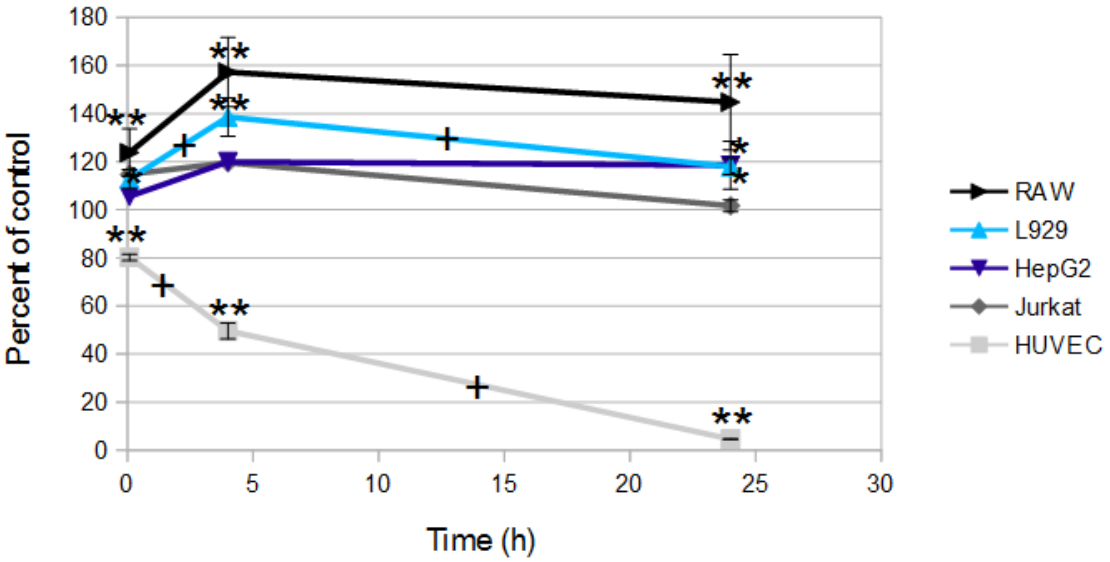


*Figure 7: CellTiter Blue viability of cells incubated with 1.8 mM Fe (SPIO) for 5 minutes, 4 hours and 24 hours, presented as mean percentage of control +/- standard deviation. Control cells for each cell line were cells treated with only $H_20$. Cells were seeded in 90 µl//well in 96-well plates, 3 replicates. CellTiter Blue was added 4 hours before measurements. Note that there is no standard deviations for HepG2 and Jurkat cells incubated with SPIO for 5 minutes and 4 hours as only 1-2 replicates were possible to create. The stars show a significant difference (*: p<0.05, **: p<0.01) compared to control. A plus sign indicates a significant (+: p<0.05, ++:p<0.01) difference between two data points.*

That the signal increase in RAW264.7 and L929 cells already after 5 minutes suggests that the SPIO particles somehow might influence the signal as 5 minutes should not be enough time to trigger an increase in metabolic activity. That the fluorescence signals in general are increased already after 5 minutes and as highest after 4 hours could mean that, in addition to slightly in some way enhance the signal, the SPIO particles also trigger an increased metabolic activity in the cells. When the cells have adapted to the presence of the particles, the metabolic activity could perhaps decreases a little, but remains elevated as seen after 24 hours.

In a previous project work at Spago Imaging AB, CellTiter Blue viability was measured on HepG2 cells incubated with PEGylated SPIO particles at the same concentrations as tested here[18]. An increase in signal was seen for lower concentrations, but not as great as here, suggesting that the PEGylated particles might interfere less with the signal and/or do not trigger an increased metabolic activity to the same extent. Olsson (2013) also reported HepG2 cells with a metabolic activity above 80% of control after 24 hours incubation with 1.8 mM Fe[18], which suggest that there could be a

negative effect on metabolic activity, but this is not seen on HepG2 cells in this report.

During the SPIO uptake tests, HepG2, L929, Jurkat and RAW264.7 cells, incubated with 0 - 0.9 mM Fe (naked SPIO) for 24 hours, were counted and the cell numbers were similar for each SPIO concentration, within each cell line (data not shown). This confirms that SPIO up to 0.9 mM is well tolerated. SPIO uptake tests were never done on HUVEC cells and they were never counted, but SPIO were used as reference in IXGp uptake test where almost all HUVEC cells had detached from the bottom of the wells after 24 hours incubation with 0.9 mM Fe (naked SPIO).

In conclusion, up to 1.8 mM Fe (naked SPIO) seems to be well tolerated by L929, HepG2, RAW264.7 and Jurkat cells and the metabolic activity might even increase. HUVEC cells, on the other hand, reacted strongly to 0.9 mM Fe by a decrease in metabolic activity down to 9% of control and detachment from the bottom of the wells. These data indicates that SPIO might be used as a reference particle for four of the cell lines. The downside is the toxicity of SPIO particles on HUVEC cells. The HUVEC cell line is especially relevant in this study as it is a human, non-immortalized endothelial cell line and thus the most representative to an *in vivo* situation in humans. Furthermore, IXGp will be in direct contact to endothelial cells while circulating in the blood. It is therefore unfortunate that SPIO particles could not be used as a reference particle for cellular uptake in HUVEC cells. Perhaps, the HUVEC cells used in this report may not have been in a good state, as they were generally more difficult to handle, for example even untreated cells loosened from the wells during washing steps. The cells used here had been bought, gone through a few population doubling times and then frozen down again. In future projects it would be advisable to directly use newly bought HUVEC cells.

### *Toxicity of IXGp*

The metabolic activity of cells treated with IXGp at 0 - 21 mM Si for 24 hours can be seen in figure 8. Up to 21 mM Si (IXGp) has no significant effect on L929, RAW264.7 and Jurkat cells. HepG2 cells treated with 1.34, 5.37 and 10.74 mM Si (IXGp) show a significant increase in fluorescence signal, suggesting an elevated metabolic activity. The signal then goes below 100% of control at 21 mM Si (IXGp), but this is not significant. The metabolic activity of HepG2 cells at 21 mM is only 76% compared to the highest fluorescence level seen at 2.7 mM, suggesting that HepG2 cells might be affected. HUVEC cells show a decrease in overall metabolic activity already at 5 mM Si and

continue do decrease to 75% of control at 21 mM Si.

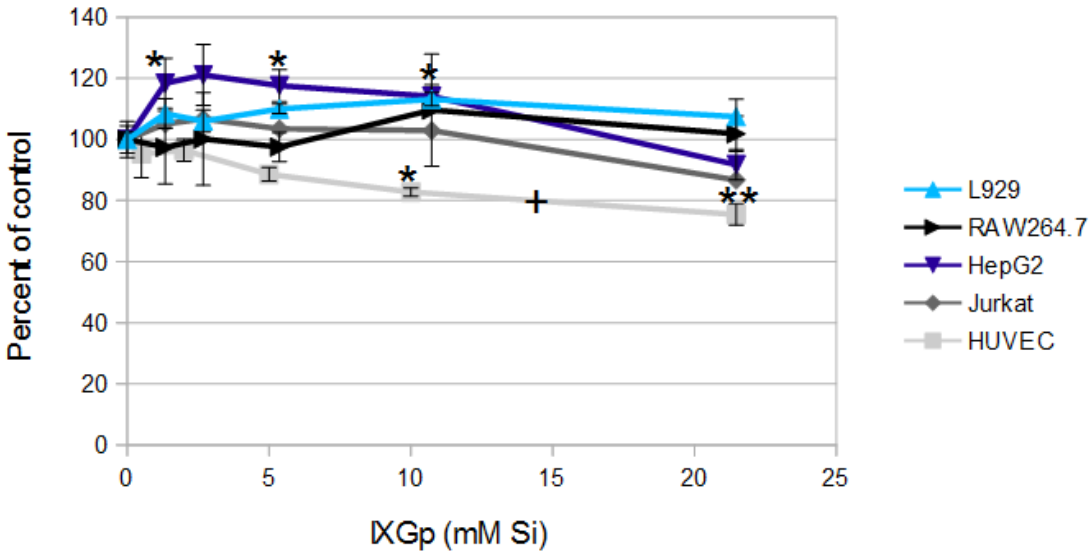


*Figure 8: CellTiter Blue viability measurements of cells treated with various concentrations of IXGp for 24 hours, presented as mean percent of control +/- standard deviation. Control cells for each cell line were cells treated with only $H_20$. Cells were seeded in 90 µl//well in 96-well plates, 3 replicates. CellTiter Blue was added 4 hours before measurements. The stars show a significant difference (*: p<0.05, **: p<0.01) compared to control. A plus sign indicates a significant (+: p<0.05, ++:p<0.01) difference between two data points.*

Previous work by Olsson (2013) investigated HepG2 cells and reported an increased CellTiter Blue fluorescence up to roughly 110% of control when the cells were treated with <5 mM Si (IXGp) and and the signal then went down to roughly 65 - 90% at 28 mM Si[18]. This is in agreement with the data reported here, but the HepG2 data in this report is shifted upwards a few percent.

In figure 9, cells incubated with 21 mM Si (IXGp) for 5 minutes, 4 hours and 24 hours can be seen. Only HepG2 cells show a significant increase in fluorescence after 5 minutes and 4 hours. HUVEC cells were significantly affected at all data points. Even if not significant in all cases, RAW264.7, HepG2 and Jurkat cells show an increase in signal after 4 hours incubation with IXGp and a lower value after 24 hours incubation which, similar to SPIO treatment, would suggest that an increase in metabolic activity has been triggered in the cells after 4 hours which then decrease after 24 hours when the cells have adapted to the particles or alternatively start to be negatively affected. The increase in fluorescence for HepG2 cells after 5 minutes suggest that IXGp also might influence the signal somehow as 5 minutes probably is not enough time for the cells to increase the metabolic activity notably.

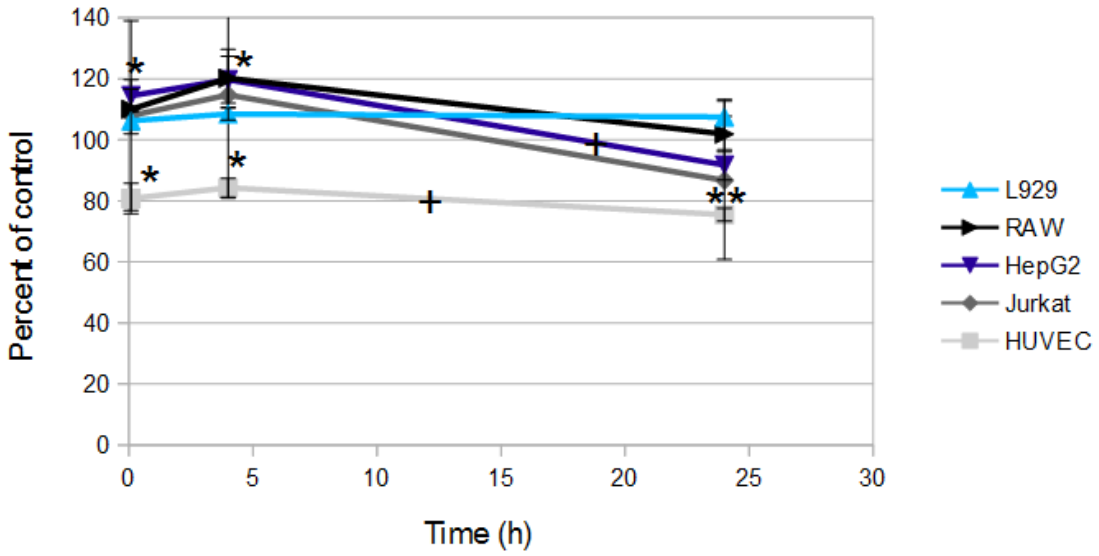


*Figure 9: CellTiter Blue viability of cells incubated with 21 mM Si (IXGp) for 5 minutes, 4 hours and 24 hours, presented as mean percent of control +/- standard deviation. Control cells for each cell line were cells treated with only $H_20$. Cells were seeded in 90 µl//well in 96-well plates, 3 replicates. CellTiter Blue was added 4 hours before measurements. The stars show a significant difference (*: p<0.05, **: p<0.01) compared to control. A plus sign indicates a significant (+: p<0.05, ++:p<0.01) difference between two data points.*

During the IXGp uptake tests, the cells were counted and in one test, HepG2, RAW264.7 and L929 cells showed similar numbers of cells when treated with either $H_2O$ or 21 mM Si (IXGp) for 24 hours. In another IXGp uptake test, the numbers were much lower compared to control, only 74, 71, 67 and 81% for HepG2, RAW264.7, L929 and Jurkat cells, respectively, when incubated with 21 mM Si (IXGp) for 24 hours. HUVEC on the other hand was very difficult to handle and many cells were lost, even control cells. Consequently, two tests resulted in 2 and 6 times as many cells after treatment with 21 mM Si compared to control. Therefore, the counted HUVEC cell numbers can not be compared to the CellTiter Blue viability tests (figure 8 and 9) as cells were likely lost due to the washing methods, not because of IXGp effects. The decrease in cell number with higher concentrations IXGp seen for the other four cell types would suggests a negative effect on the cells, but since this was not seen in all tests a negative effect can not be proven.

In conclusion, these cell lines are resistant to IXGp concentrations that are higher than clinical relevant concentrations (exact concentration is confidential), with L929, RAW264.7, Jurkat and HepG2 cells showing no significantly negative effect at 21 mM Si, even if the fluorescence signal do go down below 100% of control for Jurkat and HepG2. The HUVEC cells on the other hand decrease in metabolic activity down to 75% at 21 mM (IXGp).

The cells were also incubated with 5 mM non-electrolyte balanced IXGp particles to test if it had a greater effect on the viability. Cells treated with non-electrolyte balanced IXGp did indeed show a lower fluorescence signal (data not shown) compared to electrolyte balanced IXGp of the same concentration. Jurkat and RAW264.7 cells were considerably more affected by the non-electrolyte balanced nanomaterial with 53 and 41% metabolic activity compared to control, respectively. Jurkat cells grow in suspension and RAW264.7 cells grow partly in suspension, while the other cell lines are adherent. This signifies the importance of electrolyte balancing the final IXGp particle.

## *Uptake of SPIO Nanoparticles*

The correlation between SPIO concentrations and $T_2$ was determined with a NMR 60 μHz relaxometer (data not shown). The results was then used to calculate iron concentrations based on the $T_2$ values from the SPIO uptake tests on HepG2, Jurkat, L929 and RAW264.7. Figure 10 shows uptake of naked SPIO as nmol Fe/million cells. HepG2 show no significant uptake of SPIO particles while Jurkat, L929 and RAW264.7 show significant uptake at all concentrations but the lowest, when comparing to background values of untreated cells. RAW264.7 and L929 cells show a significant higher uptake when incubated with 0.9 mM Fe (naked SPIO) for 24 hours compared to only 10 minutes, implying that the uptake might be due to internalization. If the uptake were due to adsorption alone, uptake after 24 hour and 10 minutes would be expected to be equal since an adsorption process is reasoned to be saturated much faster than an internalization. Because the uptake after 24 hour and 10 minutes is not significantly different in Jurkat cells, adsorption rather than internalization might have occurred in these cells. The uptake at 0.9 mM Fe after 24 hours is also lower in Jurkat compared to RAW264.7 and L9292 while the uptake after 10 minutes at 0.9 mM Fe are comparably higher in Jurkat than the other three cell lines.

Over all, the trend is that the uptake increases with increasing concentration and incubation times. The mouse macrophage cells, RAW264.7 show a markedly greater uptake capacity compared to the other cell lines. If the internalization requires energy, this could explain why a greater metabolic activity was reported for RAW264.7 cells incubated with SPIO (figure 6). The RAW264.7 cells with a cell density of roughly 2 million cells/ml might be close to saturation when incubated with 0.04 mM Fe for 24 hours as there is even a small decrease in uptake when incubated with 0.9 mM Fe (figure 10).

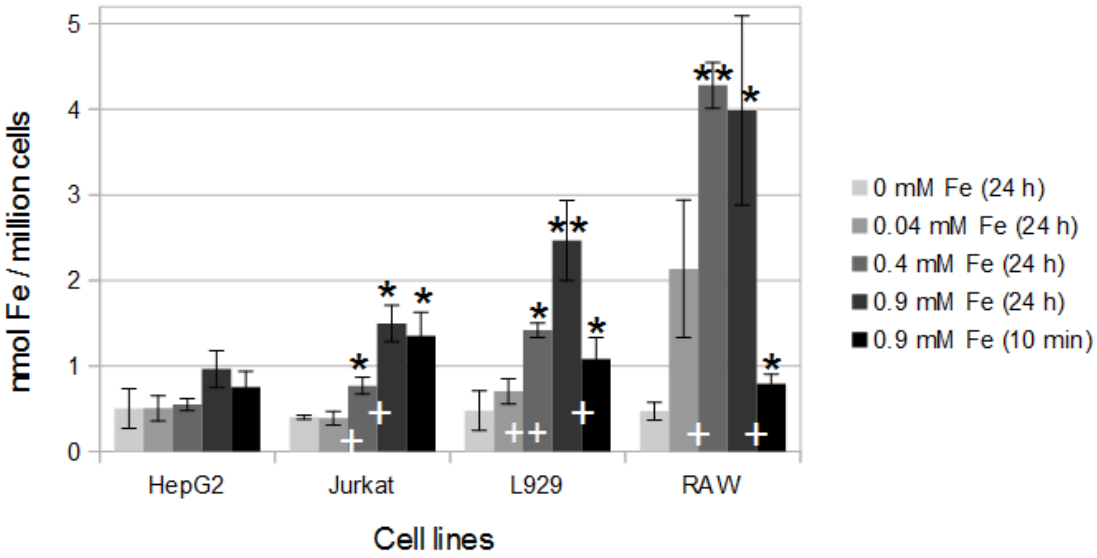


*Figure 10: Uptake of SPIO nanoparticles in different cells, presented as mean nmol Fe/million cells +/- standard deviation. Cells were incubated with various concentrations of SPIO for 24 hours or 10 minutes. Cells were seeded in 3.6 ml/well in 6-well plates, 3 replicates. The stars show a significant difference (*: p<0.05, **: p<0.01) compared to control. A plus sign indicates a significant (+: p<0.05, ++:p<0.01) difference between two data points.*

In a previous study, HepG2 and MDA-MB-231 cells were shown not to take up any particles after being incubated with 0.9 mM PEGylated SPIO particles for 10 minutes[18]. After 24 hours incubation, the HepG2 cells took up almost 20, 40 and 110 nmol SPIO/million cells[18]. This shows that PEGylated SPIO do not adhere to the cell membrane after 10 minutes and that they are internalized up to 200 times more effectively after 24 hours incubation.

SPIO uptake was also done on HepG2 cells seeded in 24-well plates instead of 6-well plates, using SPIO particles treated with PEG (figure 2, appendix 1). Note that the PEG treated SPIO particles behaved in the same way as naked SPIO particles (see section Stability of IXGp and SPIO particles) and a successful PEGylation could not be confirmed. HepG2 cells seeded in 24-well plates compared to 6-well plates appear to take up 4 times as much SPIO, when incubated with 0.9 mM Fe (PEGtreated SPIO) for 24 hours. Furthermore, there is hardly any difference in SPIO uptake between 10 minutes and 24 hours for HepG2 cells seeded in 24-well plates. However, the uptake test on HepG2 cells using 24-well plates were the first particle uptake test to be performed and the method for concentrating the cells was suboptimal with large variations making the data less reliable. Roughly only 10% of the total volume cell suspension in each test tube was taken to measure $T_2$. The actual number of cells measured with the NMR relaxometer could in fact have been higher than expected due to difficulties in mixing of the cells, which would explain the higher

values that were calculated. It can also be noted that the background values of the HepG2 cells seeded in 24-well plates were roughly 2 nmol Fe/million cells while it was only about 0.5 nmol Fe/million cells when seeded in 6-well plates (similar to the background values for the other cell types). The initial number of cells and SPIO concentration was the same for both types of wells, but the volume medium added to the wells in the 6-well plates was 4 times larger. Thus, each cell seeded in 6-well plates was exposed to up to four times as many SPIO particles, assuming equal cell doubling times. Cell counting during harvest revealed that the HepG2 cells seeded in 24-well plates had grown faster as there were only roughly 1.5 times more HepG2 cells in the 6-well plates. Since the HepG2 cells grown in 6-well plates were exposed to a higher number of SPIO particles/cell, a higher uptake is expected, but this was not the case. On the other hand, the cells seeded in 24-well plates grew faster and were perhaps more active and prone to internalize SPIO particles. Alternatively, the PEGylation could have worked to some degree, facilitating uptake, but this is contradicted by the higher uptake seen after 10 minutes.

During the IXGp uptake tests, cells were also incubated with 0.9 mM Fe (naked SPIO) for 24 hours as a positive reference. Jurkat, L929 and HepG2 cells took up 1.3, 1.6 and 2.0 nmol Fe/million cells, respectively, while RAW264.7 took up almost 15 nmol Fe/million cell. The uptake by L929 and Jurkat cells is similar to the data in figure 10, while RAW264.7 and HepG2 cells took up roughly 4 times more SPIO compared to previous trial (figure 10). Note that no SPIO background control were done as these tests were only intended as reference for IXGp uptake. A second IXGp uptake test was done on L929, HepG2 and RAW264.7 cells and the SPIO taken up here was 3.4 nmol Fe/million cells for both HepG2 and L292 and as high as 149 nmol Fe/million cell for RAW264.7. The method for concentrating these cells were more properly done and almost 100% of the cell suspension volume was analyzed, giving a more reliable result. The extremely high value seen for RAW264.7 cells, almost 40 times higher than seen in figure 10, is most likely an artifact, but further tests would be needed to confirm this. It can be mentioned that a second IXGp uptake test was also done on Jurkat cells, but was abandoned due to an extremely low cell number and thus, the SPIO uptake was never analyzed.

Percent mol iron taken up is presented in figure 3, appendix 1. The percentage uptake decreases with increasing incubation concentrations. This implies that the cells reach some level of saturation and even though they take up more mol iron when incubated with increasing concentrations SPIO, the increased concentrations of SPIO added is much higher than the resulting increase in uptake.

In conclusion, the methods used here for testing uptake of nanoparticles in cells work and the cell lines HepG2, Jurkat, L929 and RAW264.7 have a capacity to take up nanoparticles, with the RAW264.7 cells being more effective than the other cells. Furthermore, the uptake of SPIO is concentration and time dependent. Internalization of SPIO in HepG2 and Jurkat cells can not be confirmed so far, while L929 and RAW264.7 cells appear to internalize the particles.

### *Uptake of IXGp Nanoparticles*

Ideally, no cell lines should internalize the IXGp particles since they are intended to circulate in the blood stream and target tumor tissue via the EPR effect. Uptake of IXGp in HepG2, Jurkat, L929, RAW264.7 and HUVEC cell lines is presented in figure 11, as nmol Si/million cells. Data was collected from one uptake test per cell type with the exception of HUVEC cells which were pooled from two uptake tests due to low cell numbers. Note that the HUVEC cells show an artifact $H_2O$ control value of 350 nmol Si/million cells. It should also be said that analysis of silicon concentration has been difficult in this experiment with large variations and unexpectedly high negative control values as well as some low values in spiked samples. Any contact with glass is a potential source of silicon contamination and there is also a risk of silicon precipitation when the pH falls too low, making it difficult to detect the aggregated Si particles. Since the pH needs to be low during measurement, this presents a potential problem. Therefore another element or radio labeling would be advisable to use as as a tracer in future continuations on this project.

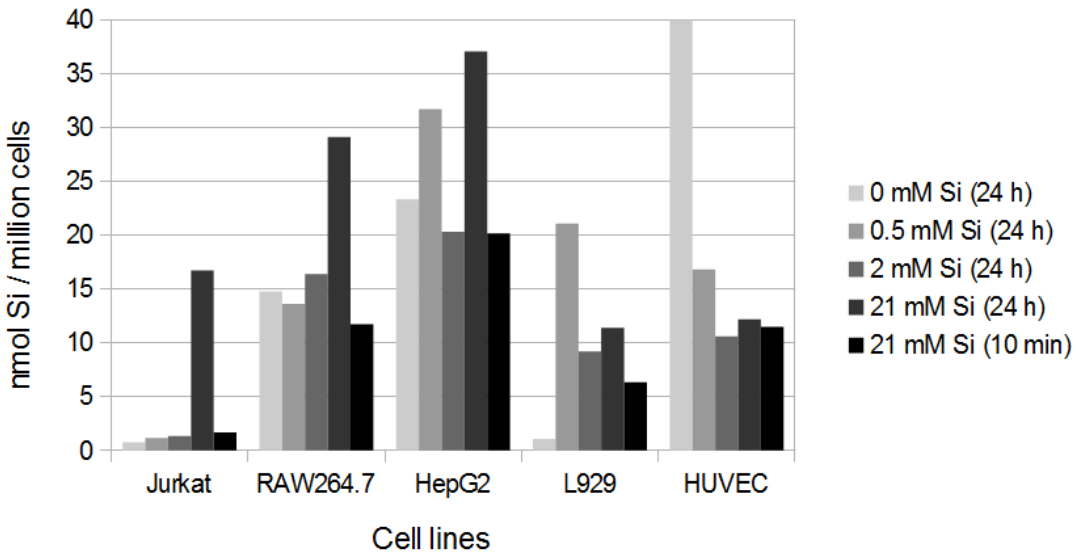


*Figure 11: Uptake of IXGp in various cell lines presented as mean nmol Si/million cells. The cells were incubated with different concentrations of IXGp for 24 hours or 10 minutes, as depicted in the legend. Cells were seeded in 3.6 ml/well in 6-well plates. 3 replicates were pooled into 1 sample due to high costs, thus no standard deviations could be calculated.*

In figure 11, Jurkat and RAW264.7 cells show a similar pattern with much higher uptake when incubated with 21 mM Si (IXGp) for 24 hours while the uptake at the other concentration is similar to respectively background values. All values, including negative control, appear to have been shifted upwards for RAW264.7 comparing Jurkat. That the uptake after 21 mM Si (IXGp) treatment for 10 minutes is similar to negative control and that the uptake after 24 hours is much higher suggests that there could be an internalization in Jurkat and RAW264.7 cells. The data could again have been slightly shifted upwards for HepG2 cells where again 21 mM Si after 24 hours show the highest value while the other incubation concentrations are similar to negative control. Though, in HepG2 the uptake is also very high already at 0.5 mM Si while it becomes lower again at 2 mM Si. Thus this makes it more difficult to trust the data in HepG2 since any of the three middle data points might be an artifact. If the data at 0.5 mM Si is an artifact, the pattern would be the same as Jurkat and RAW264.7 and an internalization might have occurred. No uptake or internalization can be concluded in L929 cells as the adsorption control with cells treated for 10 minutes are higher than negative control and value for 0.5 mM Si is much higher than all other data points. Any uptake or internalization of particles can not be seen in HUVEC cells either, especially with the extremely high water control of 350 nmol Si/million cells, making the data unreliable.

In conclusion, no IXGp internalization can be determined in HepG2, L929 and HUVEC cells, while RAW264.7 and Jurkat cells seem to internalize particles, but only at a concentration that is higher

than the intended clinical concentration (exact concentration is confidential). Olsson (2013) reported a low IXGp uptake in HepG2 cells after 24 hours incubation[18]. HepG2 cells incubated with 15 mM Si took up roughly 4 nmol Si/million cells[18], which is 3 times lower than the highest uptake seen here. Thus, cellular uptake of IXGp it likely low.

Figure 4, appendix 1 shows three other tests with IXGp in HepG2, L929 and RAW264.7 where the uptake values are much lower. HepG2 cells treated with 0.5 mM Si (IXGp) for 24 hours show an uptake of 15 nmol Si/million cell which looks like an outlier and HepG2 also generated an extremely high and unexpected value, 75 nmol Si/million cell, for the negative $H_2O$ control. However, too much focus should not be aimed at these three last tests with HepG2, L929 and RAW264.7, as they were left for a few days before being analyzed at the ICP-AES facility. During this time the Si particles could have formed precipitates if the pH fell too low during the preparations. There were also some unexpected results from control samples analyzed without cells. A sample spiked with 0.3 mM Si only showed a concentration of 2.4 μM Si and a control containing only $H_2O$ and KOH had a value of 1.9 μM Si, a similar value to cells treated with IXGp.

The percentage mol Si taken up compared to incubated mol is presented in figure 5, appendix 1 and reveal the same trend seen in the uptake test with SPIO, that the percentage is highest when incubating the cells with the lowest concentration nanoparticles and then quickly falls as the cells are incubated with higher concentrations and for shorter times.

## *Prussian Blue Staining of SPIO*

As a qualitative analysis for SPIO uptake the particles in RAW264.7 and HepG2 cells were stained with Prussian Blue, a dye that reacts with iron to give a blue color. Figure 12 shows Prussian Blue stained naked SPIO participles in HepG2 and RAW264.7 cells incubated with 0.9 mM Fe for 10 minutes and 24 hours. Negative controls are also pictured. Blue coloration can be seen in HepG2 cells incubated with 0.9 mM Fe for 24 hours (figure 12a) and it looks like the stained SPIO particles are inside the cells, suggesting that the SPIO particles have been internalized. HepG2 cells incubated with 0.9 mM Fe for 10 minutes (figure 12b) show only a few cells with blue coloration. The particles appear to be inside the cells here as well, but a bit more closer to the cell membranes. RAW264.7 cells incubated with 0.9 mM over 24 hours (figure 12d) are almost completely black with some blue coloration, confirming the SPIO uptake data (figure 10) where RAW264.7 cell are

superior in uptake capacity. When incubated for 10 minutes with 0.9 mM Fe (figure 12e) many RAW264.7 cells show faint blue coloration inside but close to the cell membranes, suggesting that some SPIO particle have adhered and/or been internalized after 10 minutes. No blue coloration can be seen when the cells were incubated with $H_2O$ (figure 12c and f).

Another Prussian Blue staining test was done were the RAW264.7 and HepG2 cells were counter stained with Neutral Red, but the counter staining made it difficult to see the blue coloration from the Prussian Blue dye. A clear uptake could still be seen for RAW264.7 cells incubated with 0.9 mM Fe (naked SPIO) over 24 hours (data not shown).

Thus, the Prussian Blue staining of naked SPIO particles confirm that SPIO particles are internalized in RAW264.7 to a great extent as seen in figure 10. The staining also conclude that the HepG2 cells do internalize SPIO particles, which could not be confirmed in figure 10 but was hinted when SPIO was used as a positive control during the IXGp uptake tests (as described in the section: Uptake of SPIO Nanoparticles). The internalization of SPIO in HepG2 and RAW264.7 cells are time dependent.

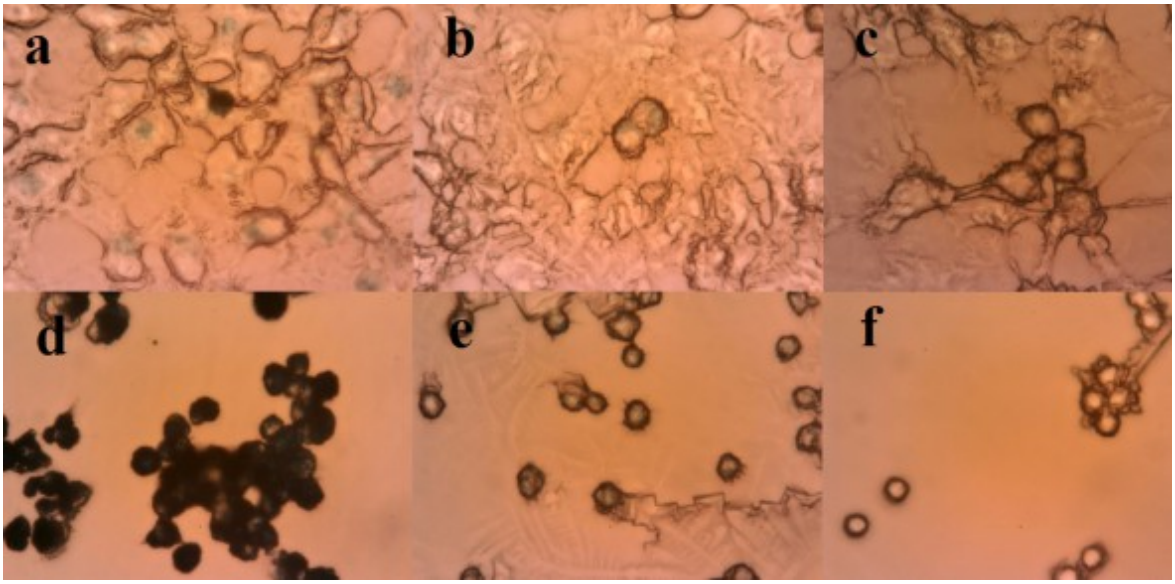


Figure 12: Prussian Blue staining of naked SPIO in HepG2 and RAW264.7 cells. **a:** HepG2 cells incubated with 0.9 mM Fe (SPIO) for 24 hours. **b:** HepG2 cells incubated with 0.9 mM SPIO for 10 minutes. **c:** HepG2 cells incubated with $H_2O$. **d:** RAW264.7 cells incubated with 0.9 mM SPIO for 24 hours. **e:** RAW264.7 cells incubated with 0.9 mM SPIO for 10 minutes. **f:** RAW264.7 cells incubated with $H_2O$.

### *Immunocytochemical Staining of IXGp*

An immunocytochemical staining was done as a qualitative test for IXGp uptake. Cells incubated with IXGp were fixated and IXGp was stained using a system with DAB, anti-PEG antibodies and horseradish peroxidase. The peroxidase produces a brown color in contact with DAB. The more IXGp particles that have been taken up, the more anti-PEG antibodies can bind to the PEG on the IXGp particles and thus more horseradish peroxidase will be present to transform DAB, giving a stronger brown color. Figure 13 shows RAW264.7, L929 and HUVEC cells incubated with 0, 0.5, 2 and 21 mM Si (IXGp) for 24 hours. It looks like there is more brown coloration when the cells are incubated with 21 mM Si over 24 hours (figure 13j-l) compared to $H_2O$ controls (figure 13a-c), suggesting that some IXGp particles are taken up. It should be said that the HUVEC cells were over all more difficult to handle in this project. Not many HUVEC cells were left after immunocytochemical staining and washing and it was especially difficult to see any cells in the negative controls. There is a large salt crystal in the middle of the negative HUVEC control and the cells in the upper corner appear to be lysed, but this was the best picture (figure 13c).

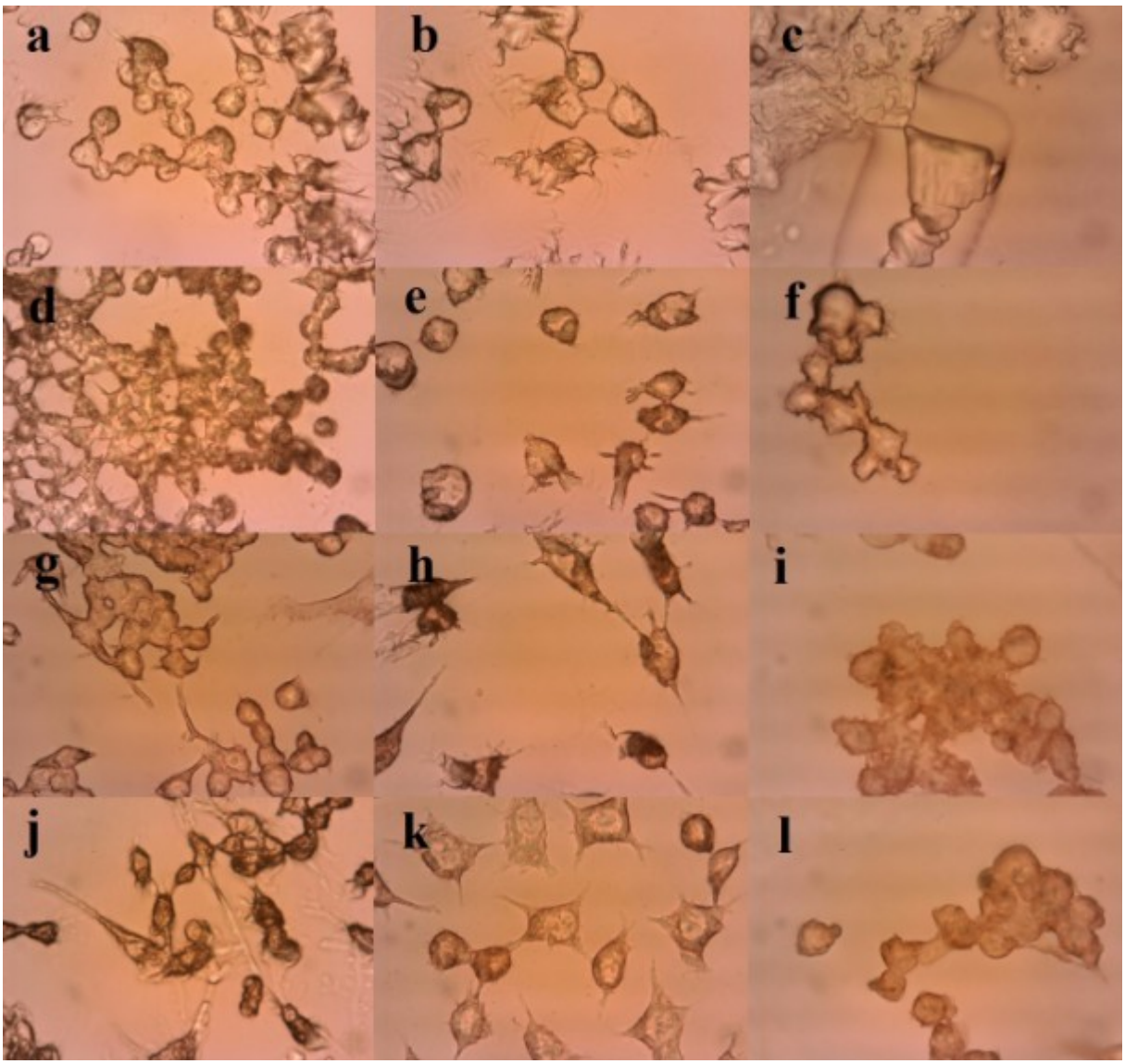


Figure 13: Immunocytochemical staining of IXGp in RAW264.7, L929 and HUVEC cells incubated with various concentrations of IXGp for 24 hours. From left to right: RAW264.7, L929 and HUVEC cells. From top to bottom: Incubated concentrations of 0, 0.5, 2 and 21 mM Si (IXGp). Note the salt crystal in the center of figure c.

There might be some indications of a concentration dependent uptake when comparing cells incubated with 0.5, 2 and 21 mM Si over 24 hours (figure 13), but the differences in color is not strong enough for a definite conclusion. The RAW264.7 cells appear darker and could therefore have taken up IXGp to a greater extent compared to the other two cell types. That the RAW264.7 cells were more effective at internalizing nanoparticles compared to the other cells were clearly seen in the SPIO uptake tests (figure 10) and Prussian Blue staining (figure 12) and to some degree in the IXGp uptake tests (figure 11).

Figure 14 shows RAW264.7, L929 and HUVEC cells incubated with 21 mM Si (IXGp) for 10 minutes (d-f) and 24 hours (g-i). Two different types of negative controls are also depicted with cells incubated with 21 mM Si for 24 hours, but without either anti-PEG antibodies or Tween 20. Without anti-PEG antibodies, the secondary antibodies conjugated to horseradish peroxidase should not be able to bind and no brown color should be produced from DAB. Figure 14a-c show that unbound secondary antibodies effectively have been removed during the washing procedure. Tween permeabilizes the cell membranes, allowing the antibodies to enter the cells and bind to IXGp within. Cells without Tween serve as a control for particle adsorption. A similar coloration with or without Tween would mean that the particles mainly adhere to the surface rather than being internalized.

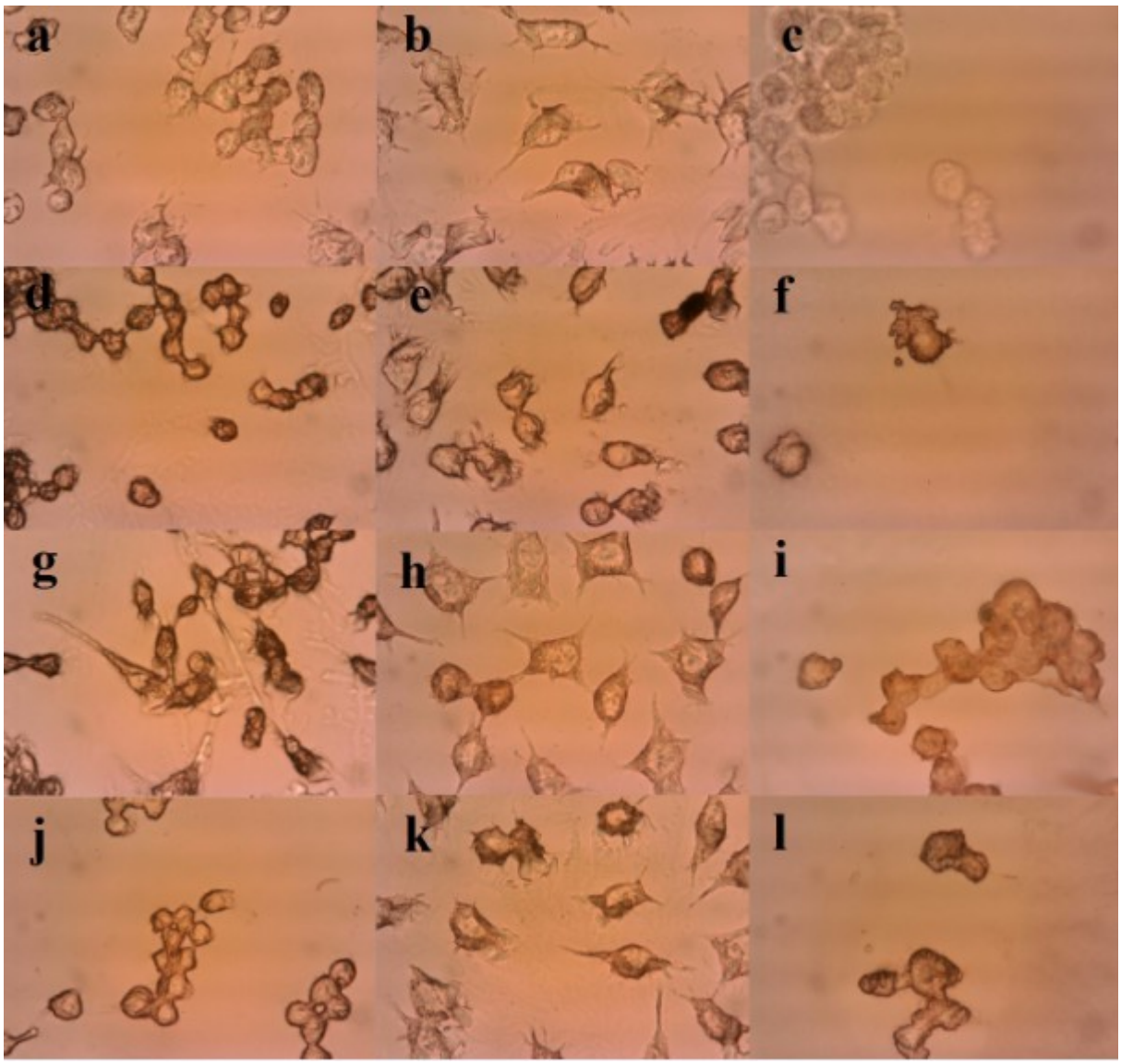


Figure 14: Immunocytochemical staining of IXGp in RAW264.7, L929 and HUVEC cells incubated with IXGp. **a-c:** RAW264.7, L929 and HUVEC cells, respectively, incubated with 21 mM Si (IXGp) for 24 hours, but without anti-PEG antibodies. **d-f:** RAW264.7, L929 and HUVEC cells, respectively, incubated with 21 mM Si for 10 minutes. **g-i:** RAW264.7, L929 and HUVEC cells, respectively, incubated with 21 mM Si for 24 hours. **j-l:** RAW264.7, L929 and HUVEC cells, respectively, incubated with 21 mM Si for 24 hours, but without Tween.

It looks like RAW264.7 cells internalize IXGp as cells treated with Tween (figure 14g) clearly show brown coloration inside the cells while cells without Tween show brown coloration only around the cells. However, L929 cells treated with or without Tween show no apparent differences. HUVEC cells treated with or without Tween are difficult to compare as there were few cells and the once seen often appeared in clumps of cells making it difficult to set the focus in the microscope.

Again, there are no clear differences when comparing cells incubated with 21 mM Si (IXGp) for 10 minutes (figure 14d-f) or 24 hours (figure 8g-i). Some slight difference might be seen in RAW264.7 where a few cells incubated for 10 minutes are less brown, suggesting a time dependent uptake of IXGp. Thus there is most likely an internalization of IXGp particles in RAW264.7 cells, but it can not be confirmed in L929 or HUVEC cells.

## Conclusions

This study shows that RAW264.7 and HepG2 cells and possibly L929 cells can internalize 10-12 nm naked SPIO particles and that the uptake is time and concentration dependent. RAW264.7 cells and possibly Jurkat cells can take up 5 nm IXGp partices, but only when incubated with concentrations higher than intended for the clinic. RAW264.7 cells were over all more effective at internalizing nanoparticles than L929, HepG2, Jurkat and HUVEC cells.

The metabolic activity of HepG2, RAW264.7, L929 and Jurkat cells were not negatively affected when incubated with up to 1.8 mM Fe (naked SPIO) or 21 mM Si (IXGp) for 24 hours. Instead, especially the RAW264.7 cells increased their metabolic activity markedly, up to 160% of control when treated with SPIO particles. HUVEC cells were over all more sensitive when handled in the tests and had a metabolic activity of 75% compared to the control, when incubated with up to 21 mM Si (IXGp) for 24 hours. The metabolic activity of HUVEC cells was reduced down to 9% and the cells detached from the surface when incubated with 0.9 mM Fe for 24 hours. The HUVEC cells might not have in a good state to begin with.

Thus, apart from the difficulties with the HUVEC cells the precursor to the contrast agent Ion-X-Gel seem to be well tolerated by L929, HepG2, Jurkat and RAW264.7 cells and appear to only be internalyzed to a very limited degree but to some greater extent by the RAW264.7 cells, not unexpected seeing as that is one of the things macrophages are designed for. This is a good indication that the final contrast agent, IXG might behave as intended, but more tests need to be done to fully evaluate the properties.

## Proposed Future Work

In future studies, it would be interesting to test more non-immortalized human cell lines, for

example HASMC and HMEC cells and see if they behave in the same way as the HUVEC cell line. It would also be interesting to further explore the time dependency. Incubation times up to 48 hours could be tested to determine when the cells reaches max uptake and the particles could be added with 30 minutes intervals during the first few hours to see when the uptake starts. If the uptake is energy dependent could be tested by incubating the cells in 4 °C to force them into growth arrest and stop the metabolic activity or by adding metabolic inhibitors to stop the production of ATP for example. If there is an energy dependance, particle internalization and adsorption could be tested by comparing the uptake in metabolically active cells with metabolically blocked cells. Uptake in tissue slices from, for example rat kidney, liver and aorta, would be interesting to study as cells in organs behave differently than in cell cultures. Further studies on the long term viability effect SPIO and IXGp have on cells could be tested by incubating cells for a few days. It would also be interesting to analyze if the viability effects is permanent or if the cells will recover when the particles are removed.

## Acknowledgments

This Master's thesis would never have been made possible without the knowledgeable personnel at Spago Imaging AB. I am truly grateful for this opportunity and all that I have learned during the past weeks. Thank you all for sharing your time and proficiency in helping me solving problems and designing experiments. I especially to thank you, Emil Aaltonen, for acting as my supervisor and constant moral support throughout this work.

## References

1. Anand, P. *et al.* Cancer is a Preventable Disease that Requires Major Lifestyle Changes. *Pharm. Res.* **25,** 2097–2116 (2008).

2. Siegel, R., Ma, J., Zou, Z. & Jemal, A. Cancer statistics, 2014. *CA A Cancer J. Clin.* **64,** 9–29 (2014).

3. Banerjee, R., Bandopadhyay, D. & Abilash, V. G. Epidemiology, Pathology, Types and Diagnosis of Soft Tissue Sarcoma: a Research Review. *Asian J. Pharm. Clin. Res.* **6,** 18–25 (2013).

4. Pautler, R. G. Mouse MRI: concepts and applications in physiology. *Physiology (Bethesda).* **19,** 168–75 (2004).

5. Storey, P. in *Magn. Reson. Imaging Methods Biol. Appl.* (Prasad, P. V) 41–42 (Humana Press Inc, 2006).

6. Jun, Y., Choi, J. & Cheon, J. Heterostructured magnetic nanoparticles: their versatility and high performance capabilities. *Chem. Commun. (Camb).* 1203–14 (2007). doi:10.1039/b614735f

7. Aime, S. *et al.* Relaxometric evaluation of novel manganese(II) complexes for application as contrast agents in magnetic resonance imaging. *J. Biol. Inorg. Chem.* **7,** 58–67 (2002).

8. Shokrollahi, H. Contrast agents for MRI. *Mater. Sci. Eng. C. Mater. Biol. Appl.* **33,** 4485–97 (2013).

9. Jokerst, J. V, Lobovkina, T., Zare, R. N. & Gambhir, S. S. Nanoparticle PEGylation for imaging and therapy. *Nanomedicine (Lond).* **6,** 715–28 (2011).

10. Greish, K. Enhanced permeability and retention effect for selective targeting of anticancer nanomedicine: are we there yet? *Drug Discov. Today. Technol.* **9,** e71–e174 (2012).

11. Spagoimaging.com. Spago Imaging AB. at <http://www.spagoimaging.com/>

12. Doiron, A. L., Clark, B. & Rinker, K. D. Endothelial nanoparticle binding kinetics are matrix and size dependent. *Biotechnol. Bioeng.* **108,** 2988–98 (2011).

13. Sabuncu, A. C. *et al.* Probing nanoparticle interactions in cell culture media. *Colloids Surf. B. Biointerfaces* **95,** 96–102 (2012).

14. Metz, S. *et al.* Capacity of human monocytes to phagocytose approved iron oxide MR contrast agents in vitro. *Eur. Radiol.* **14,** 1851–8 (2004).

15. Saito, S. *et al.* Impact of surface coating and particle size on the uptake of small and ultrasmall superparamagnetic iron oxide nanoparticles by macrophages. *Int. J. Nanomedicine* **7,** 5415–21 (2012).

16. Lorenz, M. R. *et al.* Synthesis of fluorescent polyisoprene nanoparticles and their uptake into various cells. *Macromol. Biosci.* **8,** 711–27 (2008).

17. Ma, Y., Tong, S., Bao, G., Gao, C. & Dai, Z. Indocyanine green loaded SPIO nanoparticles with phospholipid-PEG coating for dual-modal imaging and photothermal therapy. *Biomaterials* **34,** 7706–14 (2013).

18. Olsson, L. Development of an in vitro assay for analysis of cellular uptake of nanoparticles. *Masters thesis, Lund Univ. Sweden* (2013).

19. Seeliger, E., Lenhard, D. C. & Persson, P. B. Contrast Media Viscosity versus Osmolality in Kidney Injury: Lessons from Animal Studies. *Biomed Res. Int.* **2014,** 1–15 (2014).

# Appendix 1

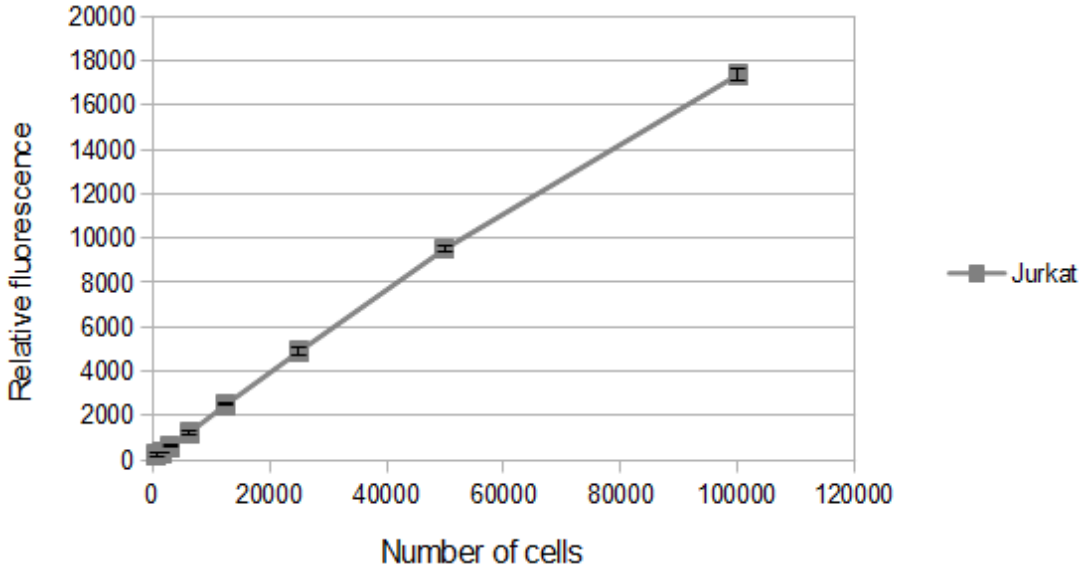


*Figure 1: Relative fluorescence versus number of cells.*

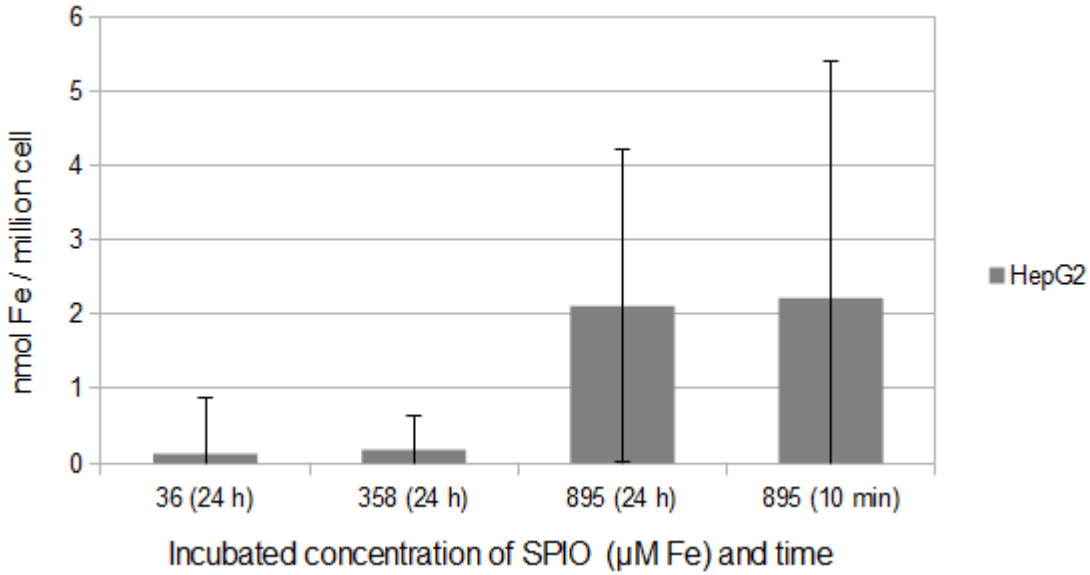


*Figure 2: Uptake of SPIO nanoparticles in HepG2 cells. 24 hours after initial seeding, cells were incubated with various concentrations of SPIO for 24 hours or 10 minutes. Data has been normalized. Cells were grown in 24-well plates.*

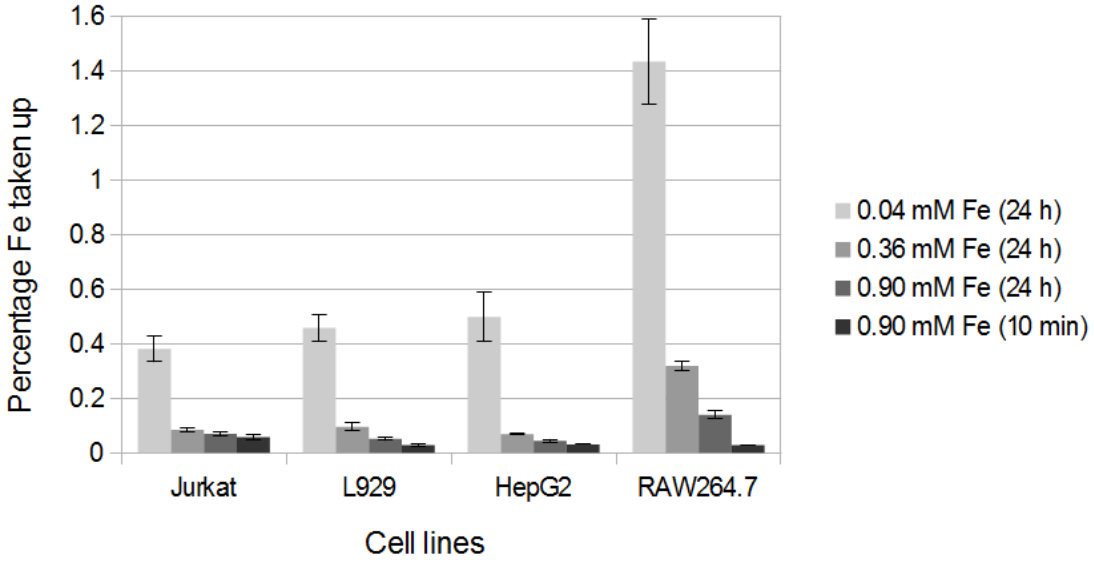


*Figure 3: Percentage mol Fe taken up in various cells treated with various concentrations of SPIO over 10 minutes or 24 hours.*

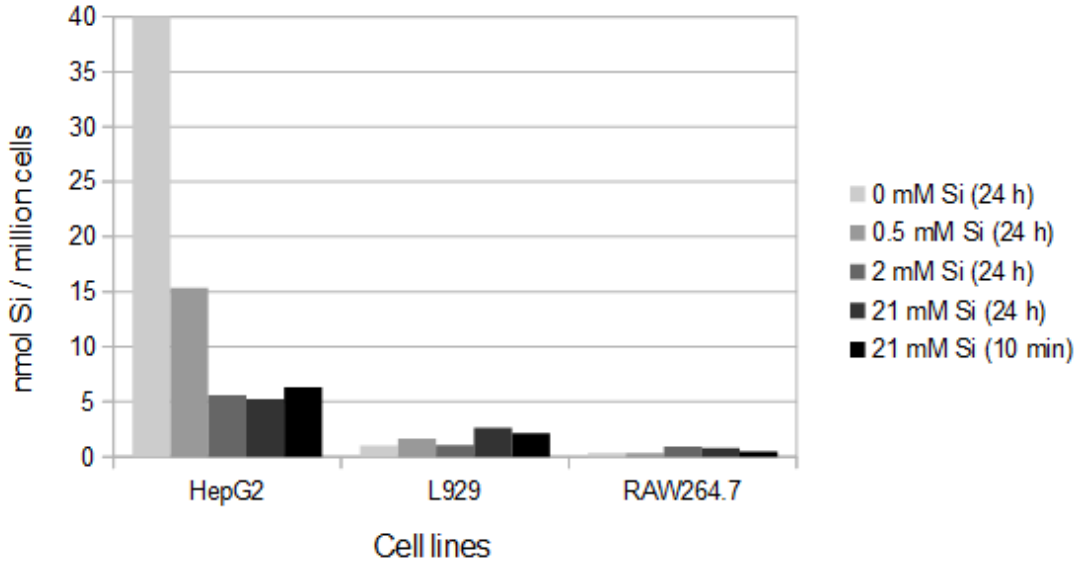


*Figure 4: Uptake of IXGp in various cell lines incubated with various concentrations of IXGp over 24 hours or 10 minutes. These data are markedly lower than seen in another setup with the same cells. Note that the negative control for the HepG2 cells fall outside the scale with a value of 75 nmol Si/million cells.*

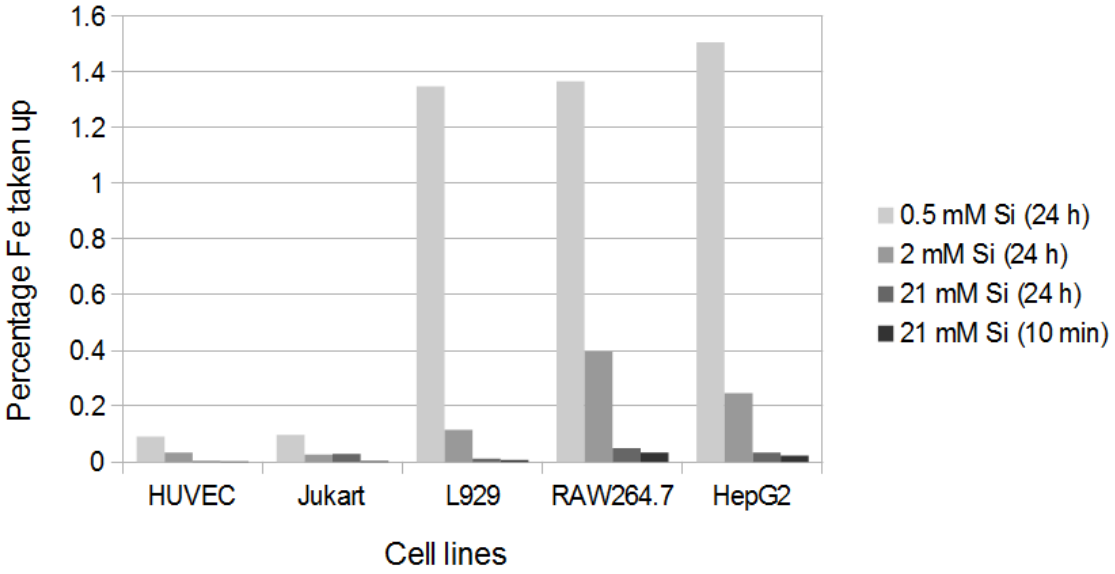


*Figure 5: Percentage mol Si (IXGp) taken up in various cells treated with various concentrations of IXGp over 10 minutes or 24 hours.*